DOCTORAL DISSERTATION

DYNAMICS AND REACTION OF GUEST MOLECULES IN $Na_3PMo_{12}O_{40}$ CRYSTAL AS STUDIED BY NUCLEAR MAGNETIC RESONANCE

A Dissertation Presented

By

SHIN' ICHI ISHIMARU

Department of Chemistry,

Tukuba University.

Submitted to the Graduate School

of Faculty of Science,

Osaka University.

in partial fulfillment of the

Doctor of Science

December, 1993

Acknowledgments

I would like to express my most sincere thanks to Professor Nobuo Nakamura for his valuable suggestions filled with his deep insight into science. Under his guidance throughout my graduate courses I could learn much about the nuclear magnetic resonance, solid state physics, and other related fields.

I wish to express my gratitude to Professor Takasuke Matuo and Professor Shichio Kawai for their critical reading of the manuscript and for their instructive comments.

I am grateful to Professor Ryuichi Ikeda for his valuable comments and continuous encouragement in writing this dissertation.

I am also very grateful to Professor Taro Eguchi, Professor Akira Inaba, Professor Wasuke Mori, and Dr. Sadamu Takeda and Dr. Hiroshi Ohki and other members of Quantum Chemistry Laboratries for their valuable discussions and numerous help in pursuing my graduate course study.

Finally, I acknowledge so much warm and encouraging guidance of Emeritus Professor Hideaki Chihara and Emeritus Professor Sigero Ikeda to the world of chemistry in my undergraduate course.

Contents

Abstract

The dynamics and the reaction of small guest molecules adsorbed in $Na_3PMo_{12}O_{40}$ crystal were investigated by solid state NMR method to clarify the catalytic mechanism of the heteropoly compound. The simplest and basic guest for this compound is water molecule; at first the dynamic property of water and deuterated water adsorbed in $Na_3PMo_{12}O_{40} \cdot nH_2O$ and $Na_3PMo_{12}O_{40} \cdot nD_2O$ was studied over wide temperature range in order to examine the nature of the guest-host interactions. The water molecules in fully hydrate materials with $n = 29$ and deuterated hydrate with $n = 20$ behave at room temperature like those in bulk water . Below room temperature four phase transitions occur in these substances and the motional freedom of water molecules are lost successively on cooling through the transition points. The motional modes of the water in each phase were assigned by the ^1H, ^2H, and ^{23}Na NMR spectra and relaxation time measurements. Elaborate dehydration brought about the hexahydrate and deuterated hexahydrate. In these materials only a restricted motion occurs from room temperature down to 120 K, suggesting that the water molecules are bound tightly t some special site or sites, far separated from each other, and there is no significant interaction between them.

The reaction of methanol adsorbed in $Na_3PMo_{12}O_{40}$ was traced by ^1H, and ^{31}P, and ^{13}C CPMAS NMR spectra. The dynamics of the adsorbed methanol and the crystal structure of the $Na_3PMo_{12}O_{40} \cdot 6CH_3OH$ is similar to the hexahydrate.

The conversion of methanol to dimethylether in $Na_3PMo_{12}O_{40} \cdot 9CH_3OH$ occurs at 570 K. The intermediate state of the reaction was revealed to be methoxy carbon bonded to the heteropoly anion. A new mechanism was proposed for catalytic dehydration of alcohol in the heteropoly compounds in the absence of acid.

1. Introduction

The heteropoly compounds have been well known for long time. Especially 12-heteropoly acids ($H_xXM_{12}O_{40}$) have well defined composition and a variety of studies has been conducted on these structures, physical properties, and especially catalytic activities so far. The structure of these heteropoly anion was clarified by Keggin by the use of powder X-ray diffraction method[1]: Twelve MO_6 octahedra surround an XO_4 tetrahedron and construct a bulky "spherical" anion (Fig. 1.1). The central hetero-atom X can be P, As, B, Si, or Ge, and the surrounding metals M, which are so-called poly-atoms, are Mo or W but a part of them can be substituted by Ti, V, Zr, *etc.* These acids are all classified to strong acid because all of x protons dissociate perfectly in aqueous solution. The salts of these heteropoly acids with large cation such as Cs^+ and ammoniums are insoluble in water although the acids themselves and the sodium salts show very high solubility. Sodium salts are also soluble in many polar organic solvents such as alcohols, ethers, acids, *etc.* The anhydrous crystals of the sodium salts can adsorb considerable amount of the solvent molecules. The anion structure, so-called the primary structure of the heteropoly compound, is not affected by the sort and the amount of the guest solvent in the crystal lattice. On the other hand the secondary structure, *i.e.*, the three dimensional arrangement of the anion, cation, and the crystallization water or other guest molecules is influenced by the sort and the amount of the guest solvent.[2,3] It is known that the adsorbed guest molecules have high mobility which is comparable to that in the bulk liquid; and the guest solvent in the crystal is so-called pseudoliquid.[4]

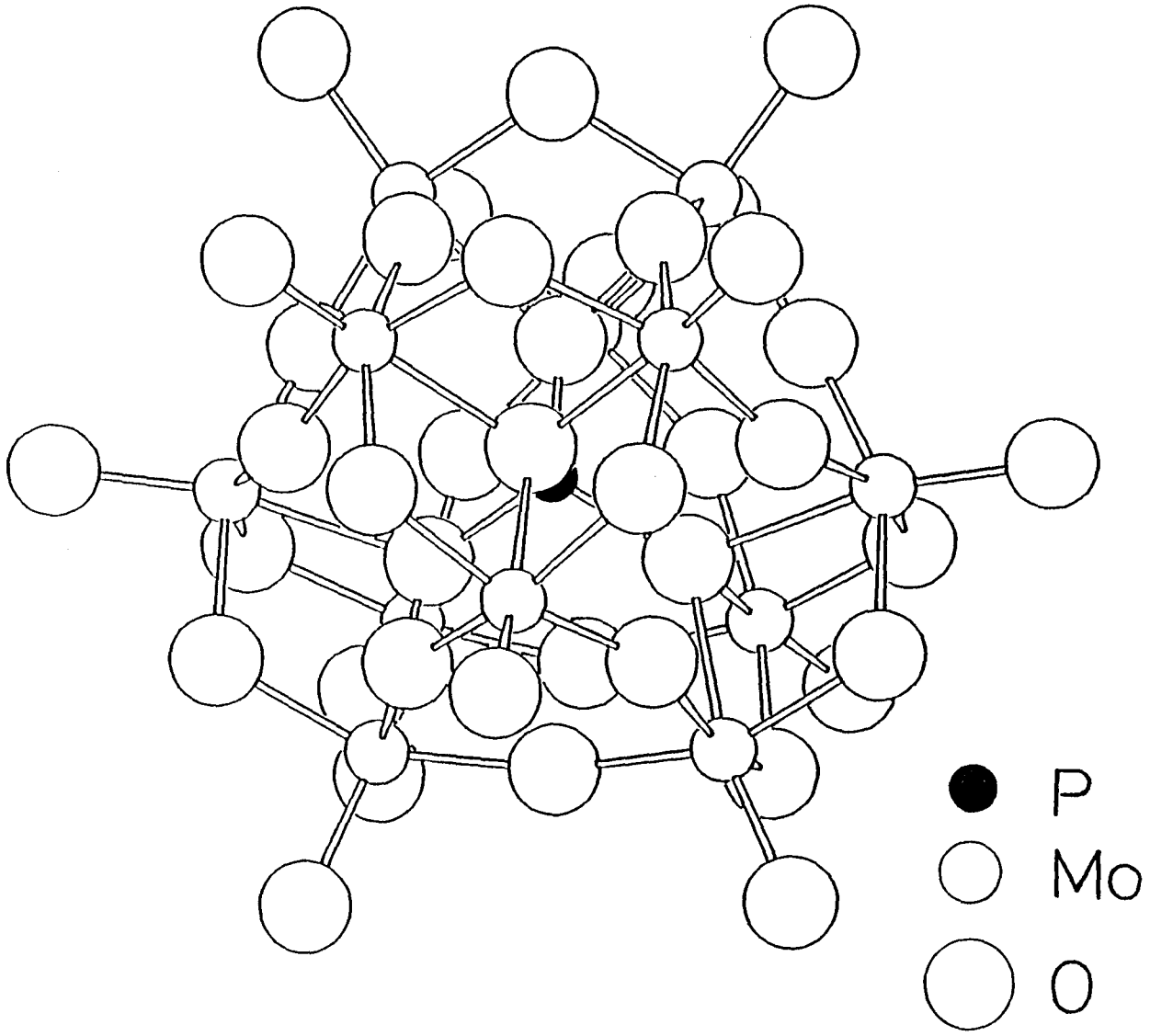

Fig. 1.1 The Keggin structure of the 12-heteropoly anion.

Recently it was found that 12-heteropoly compounds have high catalytic activity for various organic reactions such as oxidation of methacrolein[5], hydrolysis of alkenes[6], and polimerization of tetrahydrofuran. They have been used as both homogeneous and heterogeneous catalysts. The high activity and high selectivity arise from the strong acidity and oxidizing ability. Furthermore possible circulation of the pseudoliquid phase makes it possible for each guest molecule to contact to the acidic active sites, thus the effective reaction area is largely extended even in bulk solid phase. Although it is unknown that only the 12-heteropoly and its related compounds show high activity whereas other many heteropoly and isopoly compounds which have similar composition do not.

The room temperature structure and the dynamics of the water in $H_3PMo_{12}O_{40} \cdot nH_2O$ were studied by Chidichimo *et al.* using ^2H and ^{31}P NMR methods.[7,8] They stated that two orthorhombic structures exist at high water content and the acid protons penetrate into the Keggin cage. It has been known that two water molecules and the acid proton in $H_3PMo_{12}O_{40} \cdot 6H_2O$ combine to form a hydronium ion $H_5O_2^+$.[9] Slade *et al.* investigated the dynamic process of proton conduction and dynamics of the $H_5O_2^+$ ion in $H_3PMo_{12}O_{40} \cdot nH_2O$ crystals with $n = 6$ and 14 by neutron scattering and ^1H NMR.[10,11]

On the other hand the salts of the heteropoly acids have only a little studied. In the case of trisodium salt $Na_3PMo_{12}O_{40}$ it is considered that Na^+ ion in the crystal occupies the position of H^+ in the acid crystal and forms a hydrated cation. Hence the water molecules in the sodium salt are expected to behave in a quite different manner from the water in the acid because of the large size of the solvated cation. In addition, this salt has no acid

proton but shows a catalytic activity. The detail of reason for such oxidizing property has not been clarified.

It is important to examine the static and dynamical behavior of the structural water in the heteropoly compound crystal from the microscopic point of view in relation to the catalytic activity of the compounds. For this purpose nuclear magnetic resonance (NMR) on the water molecule and the cations is very effective. However most of the previous experimental works such as NMR[11,12,13], measurements of absorption-desorption process of the guest molecules[14], *etc.* on the 12-tungsto- or 12-molybdophosphoric acids and their salts have been conducted at room temperature and above. At such temperatures NMR gives information on only motionally averaged properties of the "pseudoliquid" phase. In order to obtain the information about the microscopic behavior of the structural water as well as the nature of the host-guest interaction which brings about the catalytic activity of heteropoly compounds present NMR experiments at low temperatures were conducted. The second guest material adopted in this paper for examining the catalytic reaction in heteropoly compounds is methanol which is one of the essential materials undergoing simple organic reaction; this compound thus most suitable guest to trace the reaction process in the heteropoly compounds.

In chapter **2** the results of ^{1}H, ^{2}H, and ^{23}Na NMR measurements over wide temperature range will be presented and the dynamics of the crystallization water in a representative heteropoly compound, $Na_3PMo_{12}O_{40} \cdot nH_2O$ will be discussed. Furthermore the reaction process of methanol which is the most simple organic compound absorbed in

$Na_3PMo_{12}O_{40}$ crystal is explored by solid state ^{13}C cross-polarization magic angle spinning (CPMAS) NMR and ^{1}H and ^{31}P MAS NMR. The experimental results and discussion of the reaction mechanism will be represented in chapter **3**.

References for chapter 1

[1] J. F. Keggin, *Proc. Roy. Soc.*, **A144** (1934) 75.

[2] *e.g.*, H. D'Amour and R. Almann., *Z. Kristall.*, **143**(1976)1.

[3]C. J. Clark and D. Hall, *Acta Crystallogr.*, **32**(1976)1545.

[4] M. Misono, *Catal. Rev.*, **29**(1987)269.

[5] S. Nakamura and H. Ichihashi, *Proc. 7th Intern. Congr. Catal. 1980*, Kodansha, Tokyo, 1981.

[6] Y. Onoue, Y. Mizutani, S. Akiyama, and Y. Izumi, *Chemtech.*, **8**(1987)432.

[7] G. Chidichimo, A. Golleme, D. Imbardelli, and E. Santoro, *J. Phys. Chem.*, **94**(1990)6826.

[8] G. Chidichimo, A. Golleme, D. Imbardelli, and A. Iannibello, *J. Chem. Soc. Faraday Trans.*, **83**(1992)483.

[9] G. M. Brown, M. R. Noe-Spirlet, W. R. Busing, and H. A. Levy, *Acta Crystallogr.*, **B33**(1977)1038.

[10] H. A. Pressman and R. C. T. Slade, *Chem. Phys. Lett.*,, **151**(1988)354.

[11] R. C. T. Slade, I. M. Thompson, R. C. Ward, and C. Poinsignon, *J. Chem. Soc., Chem. Commun.*, **1987**,726.

[12] J. B. Black and N. J. Clayden, *J. Chem. Soc. Dalton Trans.*, (1984) 2765.

[13] K. I. Popov, V. F. Chuvaev, and V. I. Spitsyn, *Russian J. Inorg. Chem.*, **26**(1981)514.

[14] B. K Hodnett and J. B. Moffat, *J. Catal.*, **88**(1984)253.

2. The dynamics of the water molecules

2.1 Experimental

Sodium dodecamolybdophosphate, $Na_3PMo_{12}O_{40} \cdot nH_2O$, was purchased from Wako Pure Chemical Co. Ltd. The water content of this material as received was determined gravimetrically. Approximately 500 mg of the bright yellow small crystals were placed in a glass weighing bottle and heated at 620 K for 4h. The weight loss attributed to the desorption of crystallization water. The water content was determined to be $n = 29$. This is the value of the fully hydrated material.

Samples as received and dehydrated *in vacuo* at room temperature were powdered and used for the ^1H and ^{23}Na NMR measurements. The water content of latter was determined to be $n = 6$ by the gravimetric method. Deuterated specimen was prepared by repeated recrystallization from 99.9% heavy water (Aldrich). The extent of deuteration is higher than 99%. The product had the composition, $Na_3PMo_{12}O_{40} \cdot 20D_2O$. This sample and the sample dried *in vacuo* in which $n = 6$ were used for the ^2H NMR measurement. Hereafter we call the substances as follows:

29-hydrate: $Na_3PMo_{12}O_{40} \cdot 29H_2O$

hexahydrate: $Na_3PMo_{12}O_{40} \cdot 6H_2O$

deuterated 20-hydrate: $Na_3PMo_{12}O_{40} \cdot 20D_2O$

deuterated hexahydrate: $Na_3PMo_{12}O_{40} \cdot 6D_2O$

The ^1H spin-lattice relaxation time, T_1, was measured by using a MATEC 5100

spectrometer at ^{1}H Larmor frequency of 18.1 MHz between 170 and 340 K in the heating direction. All other NMR measurements were carried out by a Bruker MSL−200 NMR system with the Larmor frequencies of 200.14, 30.7, and 52.94 MHz for ^{1}H, ^{2}H, and ^{23}Na, respectively. The quadrupole echo sequence was used for the ^{1}H and ^{2}H spectrum measurements. All T_1's were measured by 90°-τ-90° and/or 180°-τ-90° pulse sequence.

The accuracy in the temperature measurements was ±0.1 K for the proton T_1 measurement and ±1 K for other measurements. The uncertainty in the relaxation times was estimated to be within 10 % in all measurements.

Differential thermal analysis (DTA) was also conducted on the hydrates with $n = 29$ and 6 (hereafter abbreviated as 29-hydrate and hexahydrate, respectively) and deuterated hydrate specimen with $n = 20$ (deuterated 20-hydrate) to examine the phase transitions.

X-ray diffraction was carried out on powdered specimens by Rigaku diffractmeter at room temperature.

2.2 Results

2.2.1 X-ray diffraction and DTA

DTA measurement on the 29-hydrate revealed that there exist four phase transitions at 257 K and at about 190 K, 180 K, and 170 K in the heating direction. The DTA peaks of the lower three transitions overlapped each other and therefore the uncertainty in the transition temperatures was large (±3K). The highest transition showed a thermal hysteresis of *ca.* 10 K, indicating that this transition is of first order. The five phases will be named Phases I, II, III, IV, and V in the order of decreasing temperature. Deuterated 20-hydrate undergoes similar transitions at about 260 K, 220 K, 200 K, and 190 K. These five phases will be defined as Phases I, II, III, IV, and V in the similar way to the 29-hydrate. The protonic hexahydrate showed no evidence for any phase transition between 77 K and 300 K.

Fig. 2.1-4 shows the powdered X-ray diffraction (XRD) patterns of the four substances at room temperature. The patterns of the 29-hydrate and the deuterated 20-hydrate resemble each other. From this fact and by taking account of the fact that trisodium 12-molybdophosphate contains unstructured water at high hydration level [13] it can be considered that the 29-hydrate and the deuterated 20-hydrate assume similar structure to each other. On the other hand, both hexahydrates, the protonic and the deuterated, give almost the same pattern which is however largely different from that of the 29-hydrate. The reflections were broad and weak at high angles and could not be observed at the angle $2\theta \geq 40°$, suggesting that the dehydration process brought about a large number of

SAMPLE NAME: Na3PMo1204
TARGET : Cu
VOL and CUR: 40KV 40mA
SLITS : DS 1 RS .3 SS 1
SCAN SPEED: 3 DEG/MIN.
STEP/SAMPL.: .02 DEG
PRESET TIME: 0 SEC
FILE NAME : NAPM100
OPERATOR : YAMAMOTO
COMMENT :

DATE: 91.05.30

SMOOTHING NO.: 11
THRESH. INTEN.: 83 CPS
2nd DERIV.: 263 CPS/(DEGxDEG)
WIDTH: .09 DEG
B.G.REDUCTION: NO EXECUTION
OUTPUT FILE :

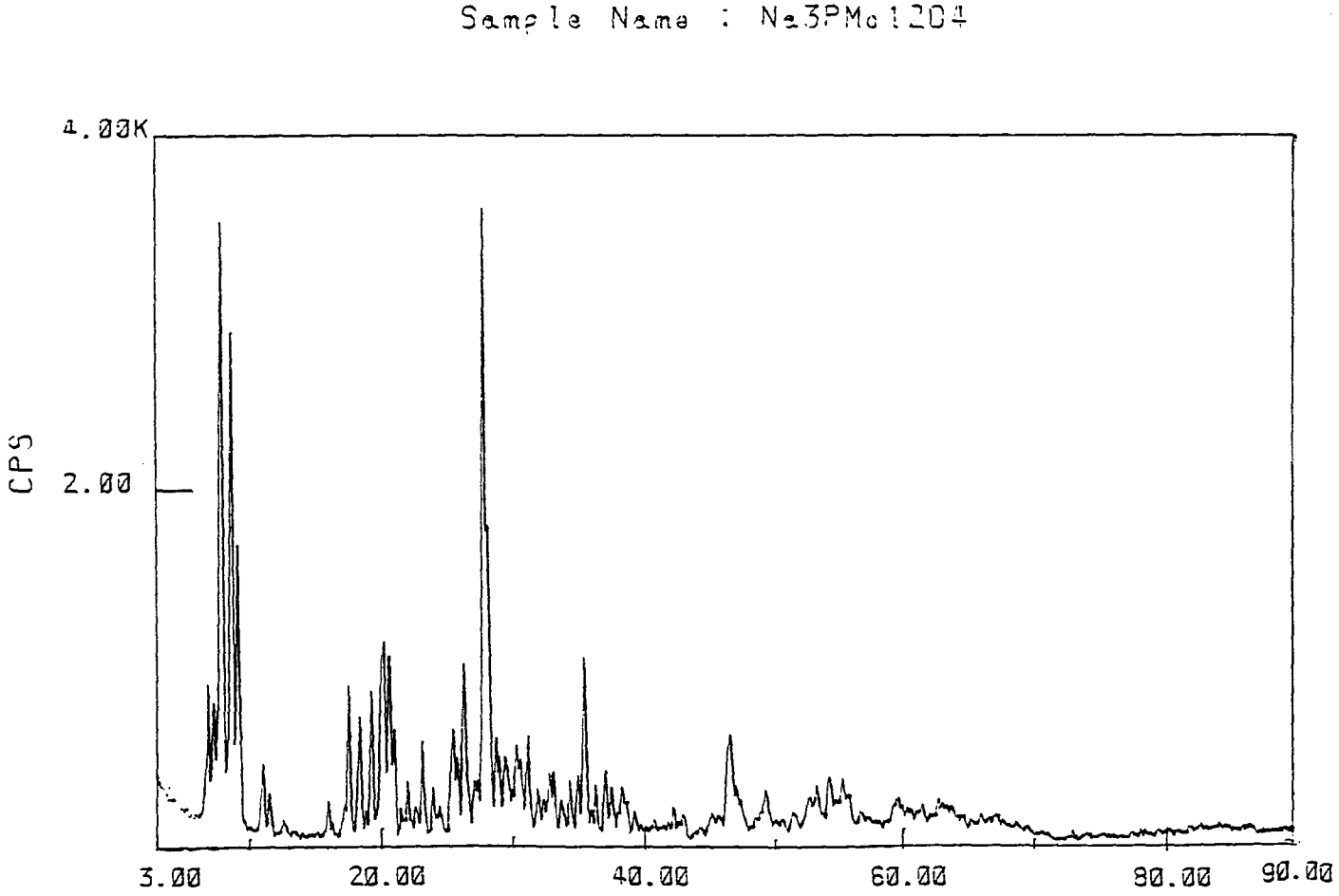

Fig. 2.1 The powder XRD patterns of $Na_3PMo_{12}O_{40} \cdot 29H_2O$ at room temperature.

SAMPLE NAME:PMo.D
TARGET :Cu
VOL and CUR: 40KV 40mA
SLITS :DS 1 RS .3 SS 1
SCAN SPEED: 3 DEG/MIN.
STEP/SAMPL.: .02 DEG
PRESET TIME: 0 SEC
FILE NAME :IS03100
OPERATOR :YAMAMOTO
COMMENT :

DATE:92.12.16

SMOOTHING NO.: 13
THRESH.INTEN.: 73 CPS
2nd DERIV.: 111 CPS/(DEGxDEG)
WIDTH: .11 DEG
B.G.REDUCTION:NO EXECUTION
OUTPUT FILE :

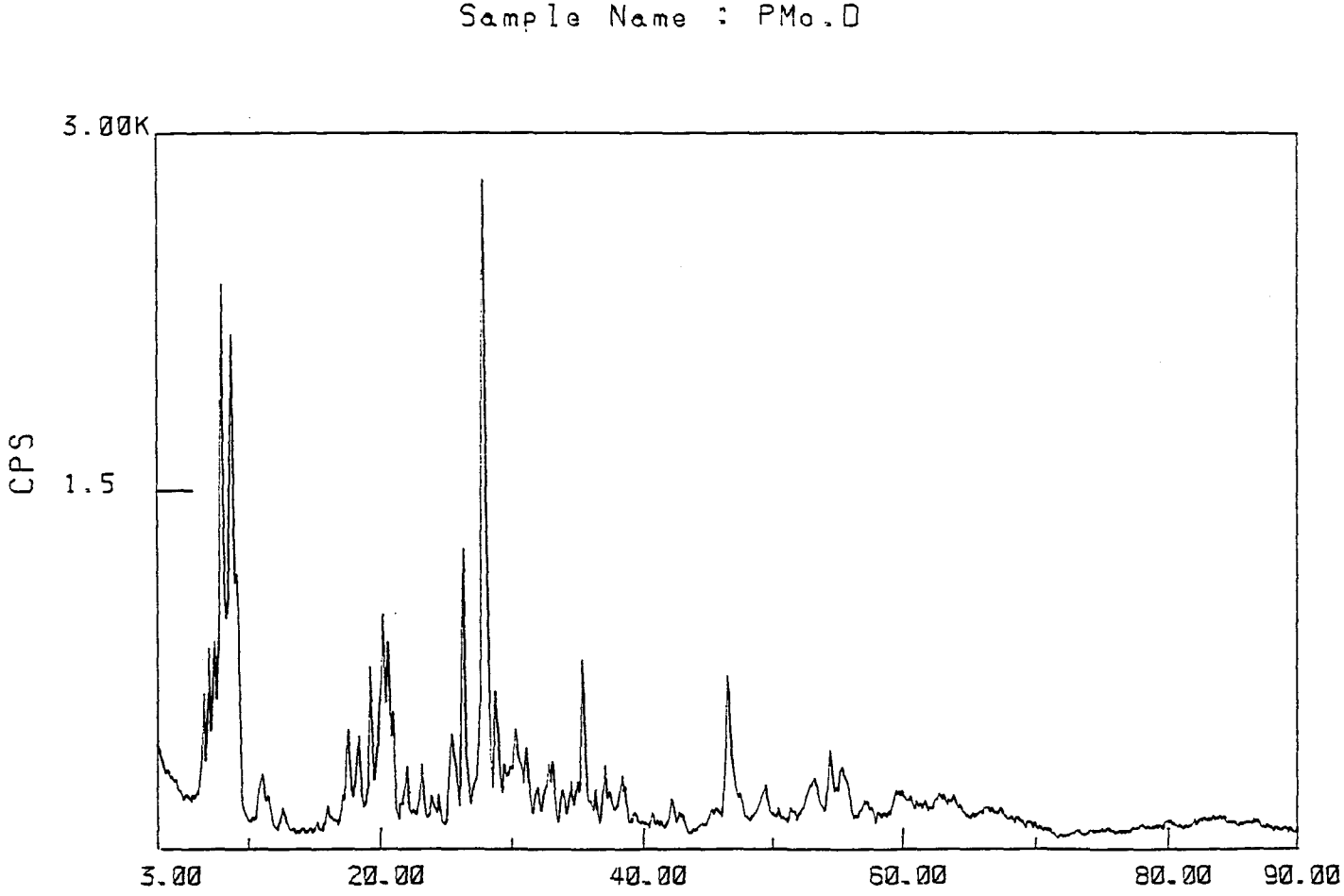

Fig. 2.2 The powder XRD patterns of $Na_3PMo_{12}O_{40} \cdot 20D_2O$ at room temperature.

SAMPLE NAME: PMo-H2O
TARGET : Cu
VOL and CUR: 40KV 40mA
SLITS : DS 1 RS .5 SS 1
SCAN SPEED: 3 DEG/MIN.
STEP/SAMPL.: .02 DEG
PRESET TIME: 0 SEC
FILE NAME : IS01100
OPERATOR : YAMAMOTO
COMMENT :

DATE: 92.10.22

SMOOTHING NO.: 13
THRESH. INTEN.: 75 CPS
2nd DERIV.: 111 CPS/(DEGxDEG)
WIDTH: .11 DEG
B.G. REDUCTION: NO EXECUTION
OUTPUT FILE :

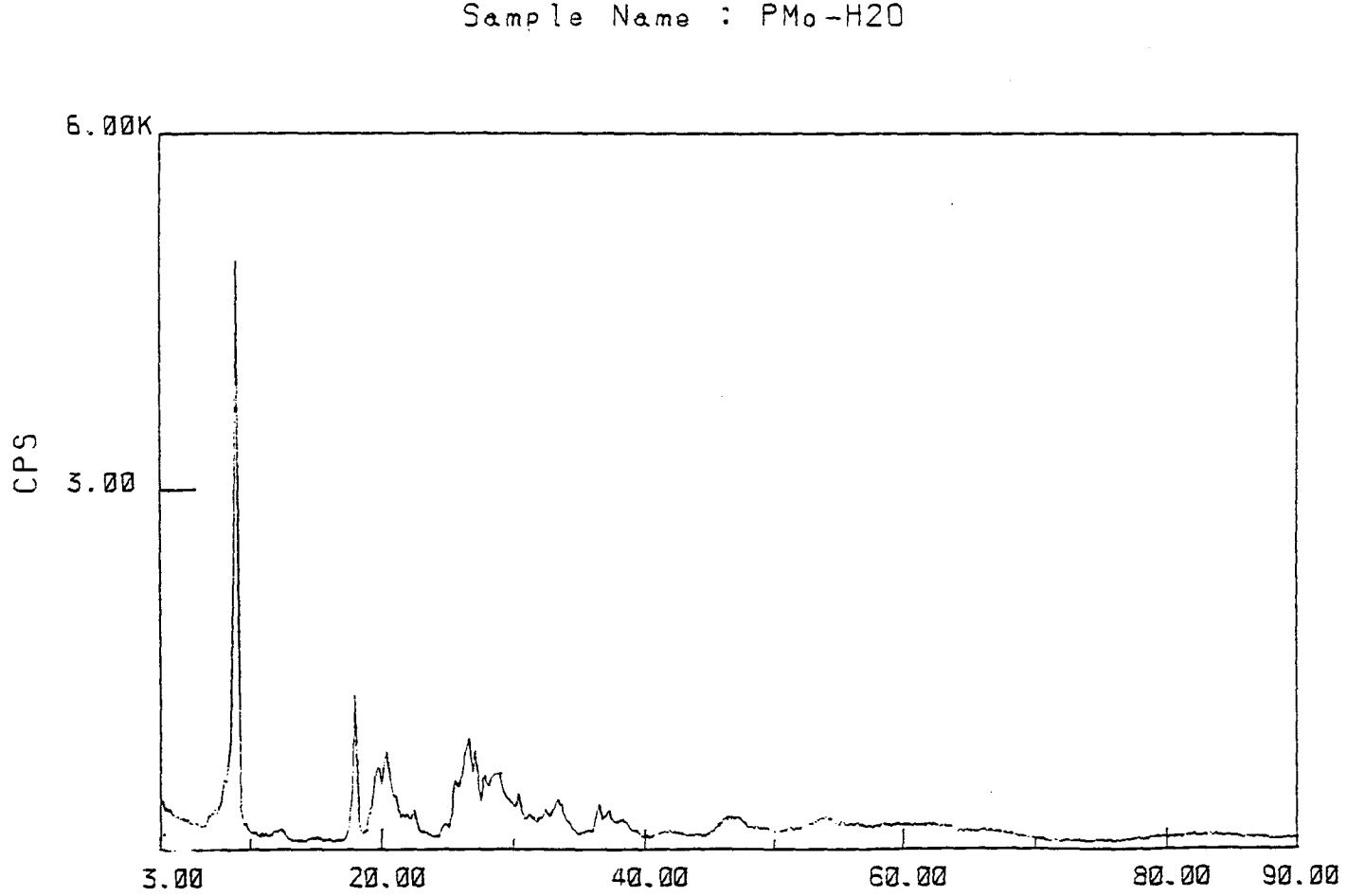

Fig. 2.3 The powder XRD patterns of $Na_3PMo_{12}O_{40} \cdot 6H_2O$ at room temperature.

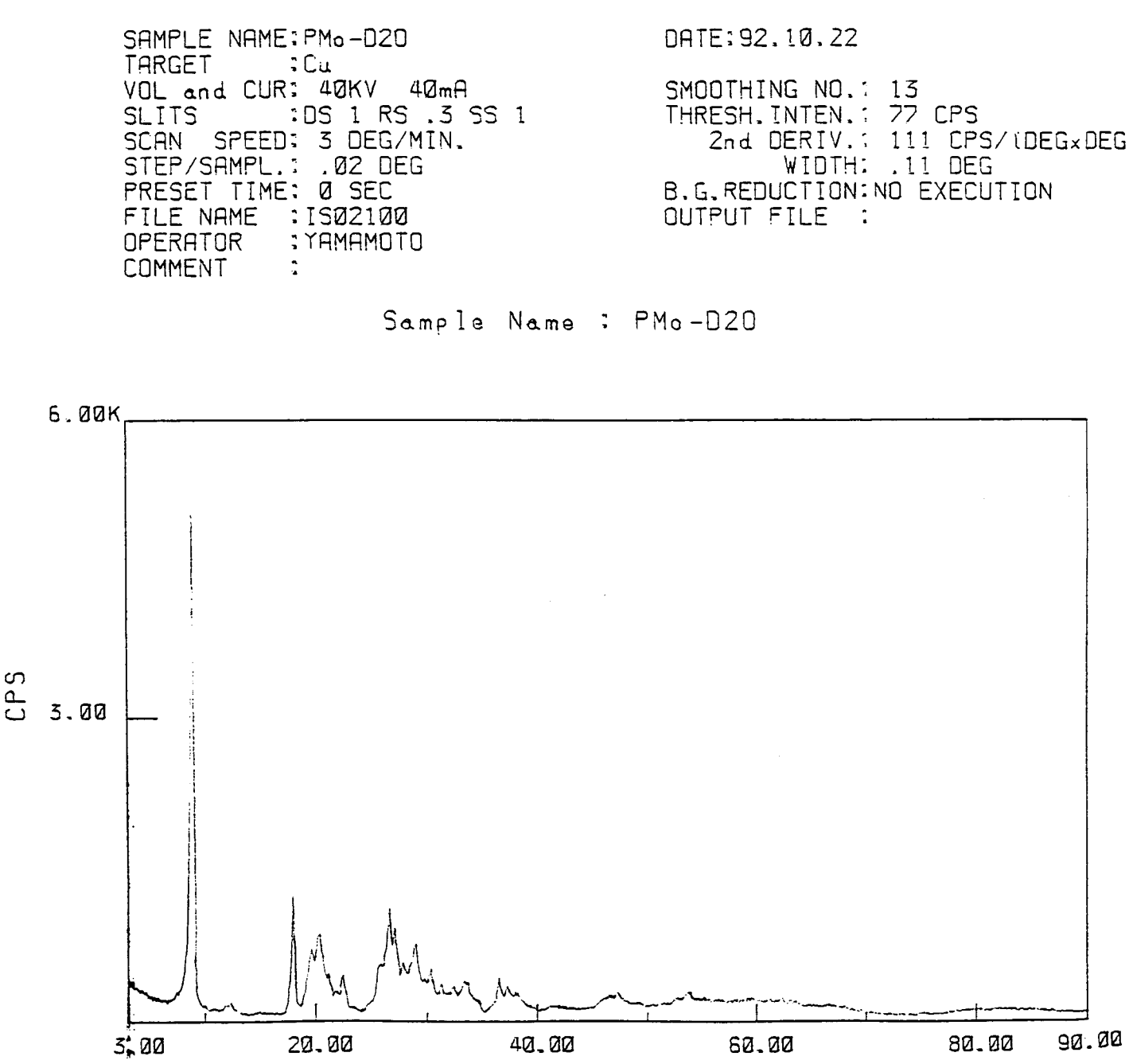

Fig. 2.4 The powder XRD patterns of $Na_3PMo_{12}O_{40} \cdot 6D_2O$ at room temperature.

imperfections into the crystal lattice. This point of view may be supported by a fact that the specimen with lower water content gives broader line in ^{31}P NMR [6] because such broadening comes usually from the broad distribution of the chemical shift due to lattice distortion.

2.2.2 ^{1}H NMR

The temperature dependence of the ^{1}H NMR spectrum of the 29-hydrate is shown in Fig. 2.5. At room temperature and up to 350 K the spectrum shows a simple sharp Lorentzian peak with the full width at half maximum(FWHM) of 270 Hz. This line shape remains unchanged down to 210 K. Below 200 K the line becomes broader steeply and another very broad component grows on cooling, the latter being characteristic of a two-spin Pake pattern.[1] In other words, two kinds of water exist in the crystal below 200 K.

On the other hand the hexahydrate gives a spectrum which is broad and consists of more than one component even at room temperature (Fig. 2.6), but the spectrum becomes sharper at higher temperatures. At low temperatures the spectrum consists of a broad single line and a distinct Pake pattern the width of which is about $\frac{2}{3}$ of that in the 29-hydrate.

Fig. 2.7 shows the temperature dependence of ^{1}H T_1 of the 29- hydrate at 18.1 MHz. In the lowest temperature phase (Phase V), the free induction decay (FID) signal was too short to determine the T_1 value. Heating the sample up to Phase IV (at 172.5 K) the FID

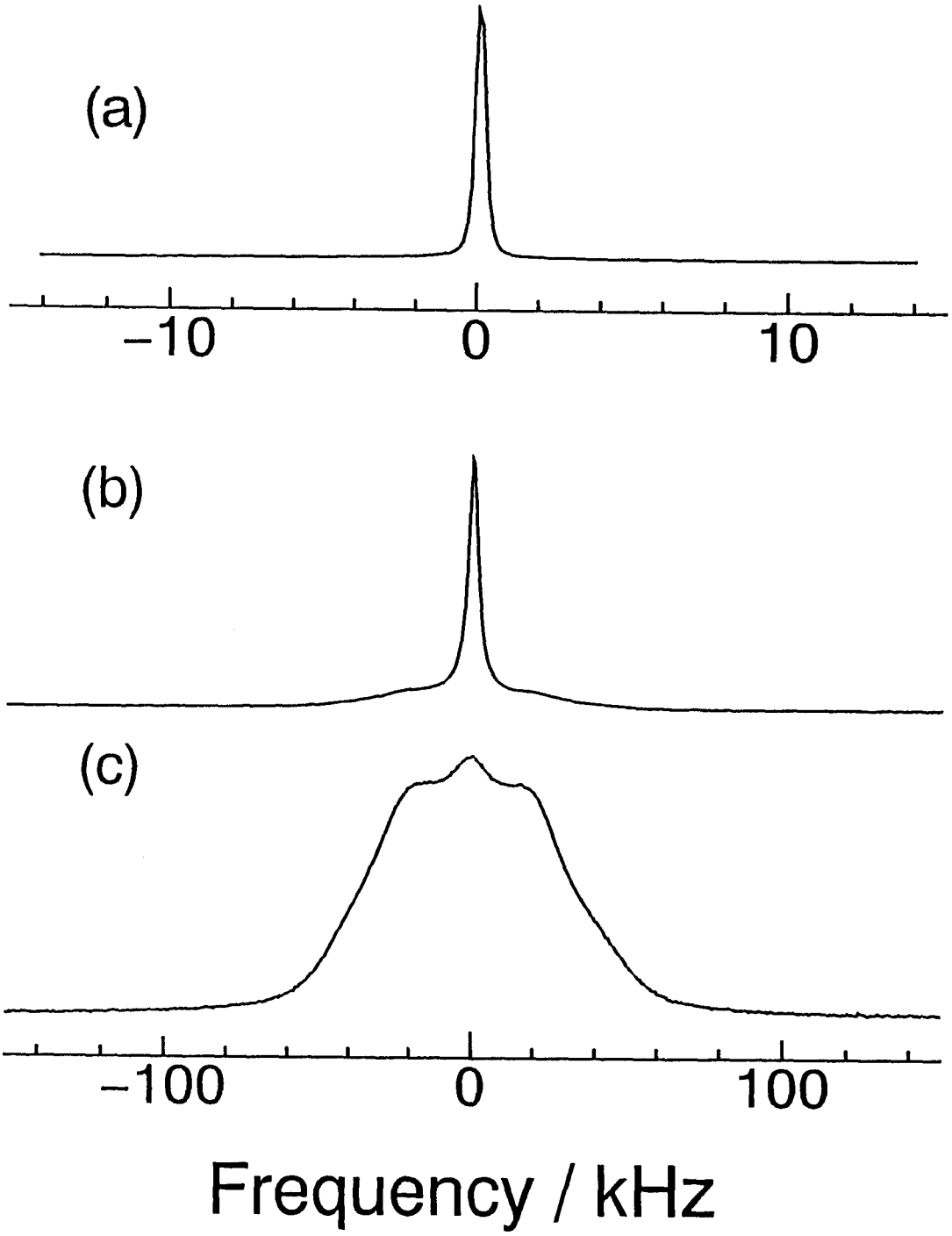

Fig. 2.5 The ^{1}H NMR spectrum of $Na_3PMo_{12}O_{40} \cdot 29H_2O$ at (a) 209 K, (b) 180 K, and (c) 150 K.

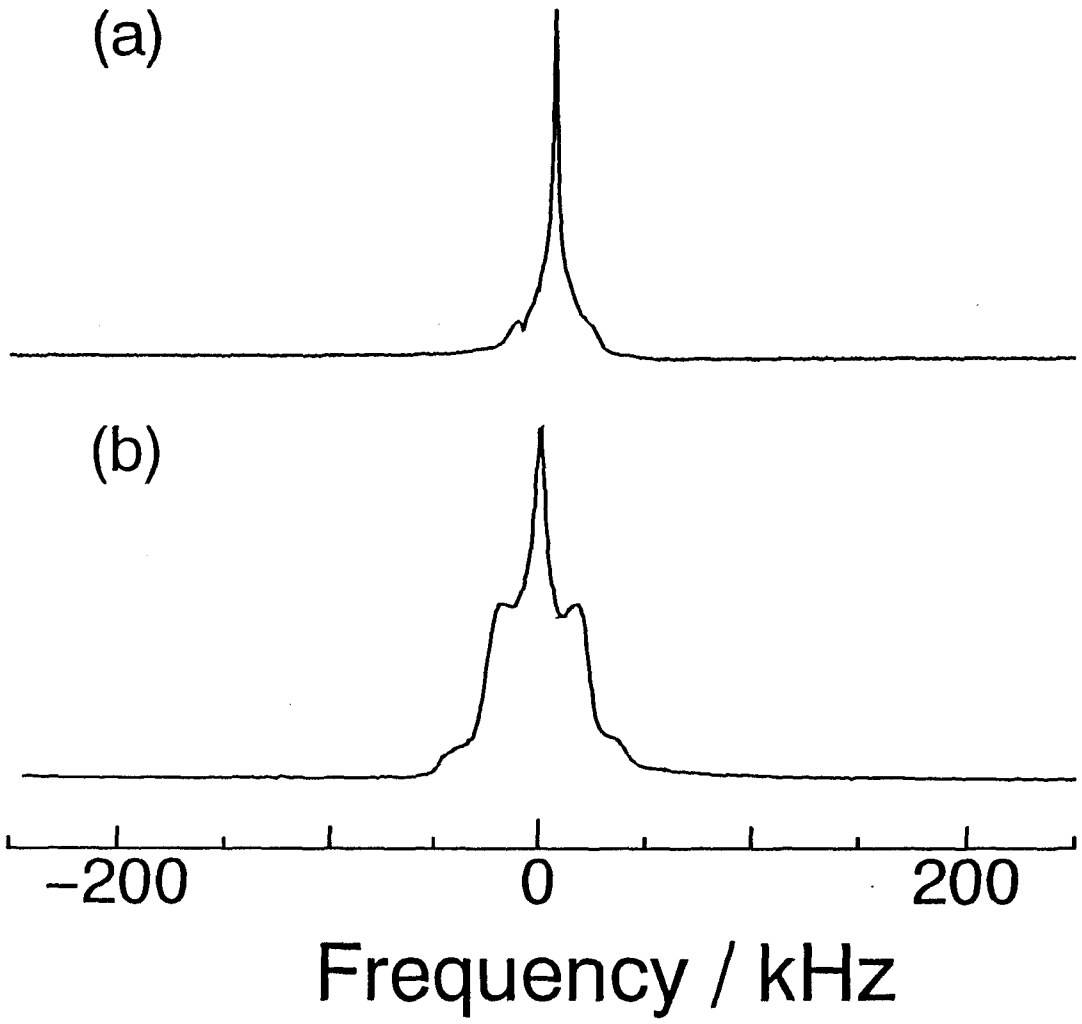

Fig. 2.6 The ^1H NMR spectrum of $Na_3PMo_{12}O_{40} \cdot 6H_2O$ at (a) room temperature and (b) 180 K.

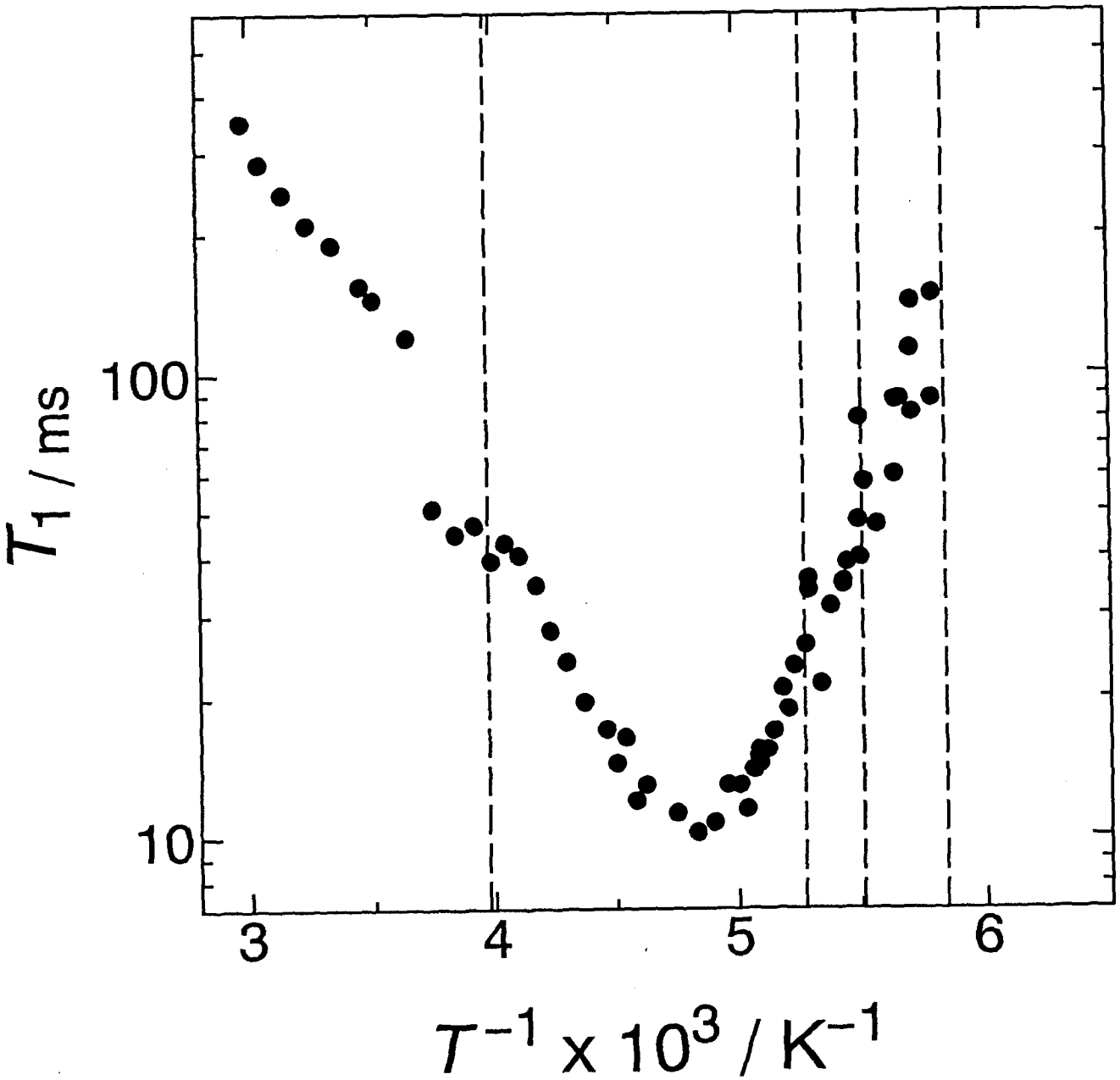

Fig. 2.7 The temperature dependence of ^1H T_1 of $Na_3PMo_{12}O_{40} \cdot 29H_2O$. The phase transition temperatures determined by DTA are shown by broken lines.

became longer than 100 μs and T_1 became measurable. On farther heating the T_1 became short and again the FID became suddenly longer at 182 K and above. However, the T_1 did not show any discontinuity at 182 K. The T_1 assumed the minimum value of 11 ms at about 207 K. At 270 K a discontinuous jump of T_1 was observed. These temperatures, 172.5 K,182 K, and 270 K, correspond obviously to three of the four phase transition temperatures.

2.2.3 ^{2}H NMR of 20- and hexahydrates

Fig. 2.8 and 2.9 show the ^{2}H NMR spectra of the deuterated 20-hydrate and the deuterated hexahydrate, respectively. The ^{2}H spectrum of the 20-hydrate may be compared with the ^{1}H spectrum of the 29-hydrate (fig. 2.8): An extremely narrow peak was observed at room temperature and it broadened out to give two components below 220 K, *i.e.*, the broad central peak and outer one characteristic of significant quadrupole interaction. However, while the central component of the ^{1}H spectrum of the 29-hydrate is a simple Lorentzian, the ^{2}H spectrum of the 20-hydrate gives a broad, indistinct central component at low temperatures. In the case of the hexahydrate the existence of two components are discernible even at room temperature and the spectrum at low temperature consists of several components (see in fig. 2.9).

Fig. 2.10 shows the temperature dependence of the ^{2}H T_1 and T_2^* (inverse line width) in the deuterated 20-hydrate. The recovery of the ^{2}H magnetization was non-exponential and could be represented by the superpositions of two relaxation process below 200 K. And

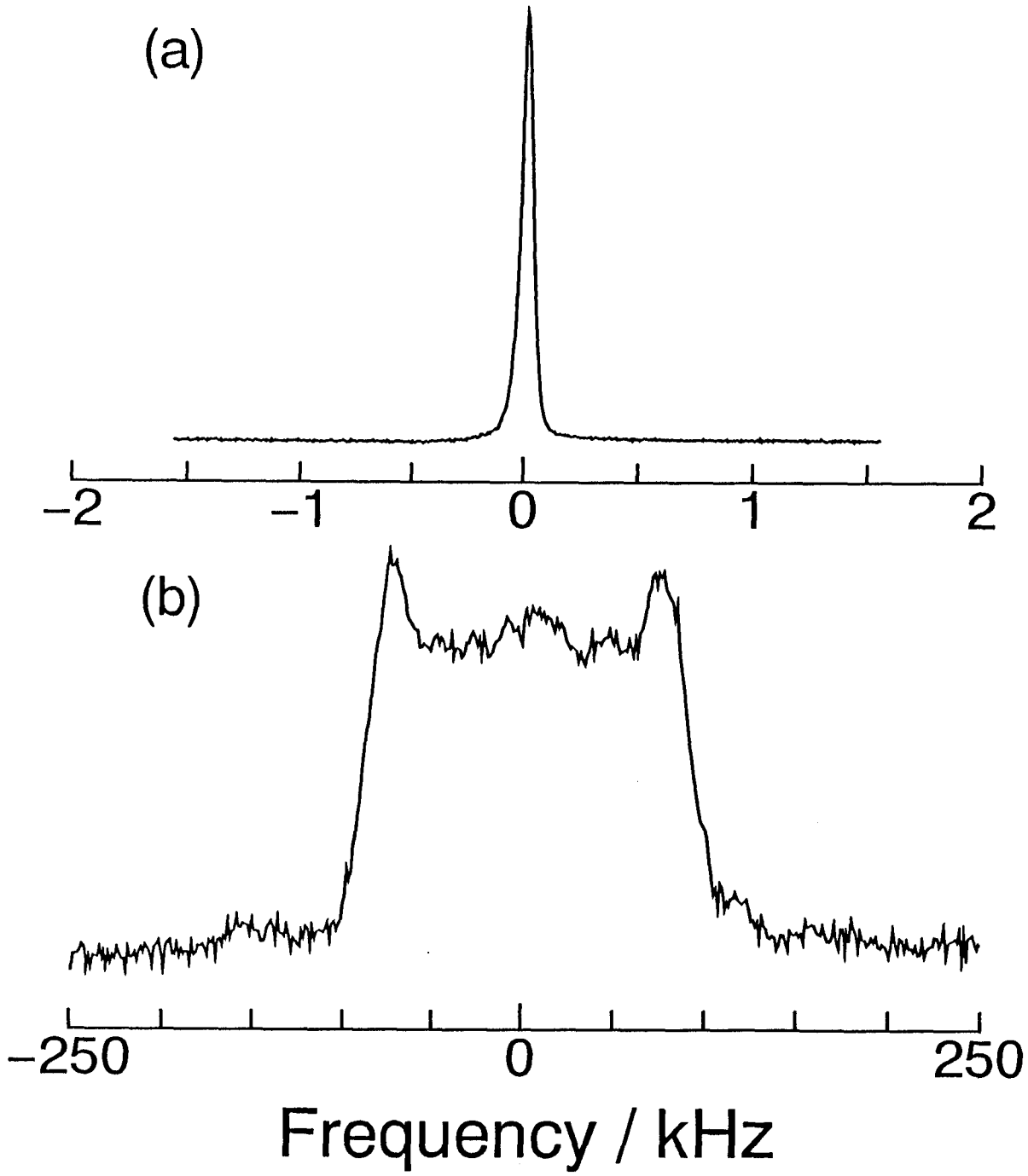

Fig. 2.8 The ^2H NMR spectra of $Na_3PMo_{12}O_{40} \cdot 20D_2O$ at (a) 300 K and (b) 120 K.

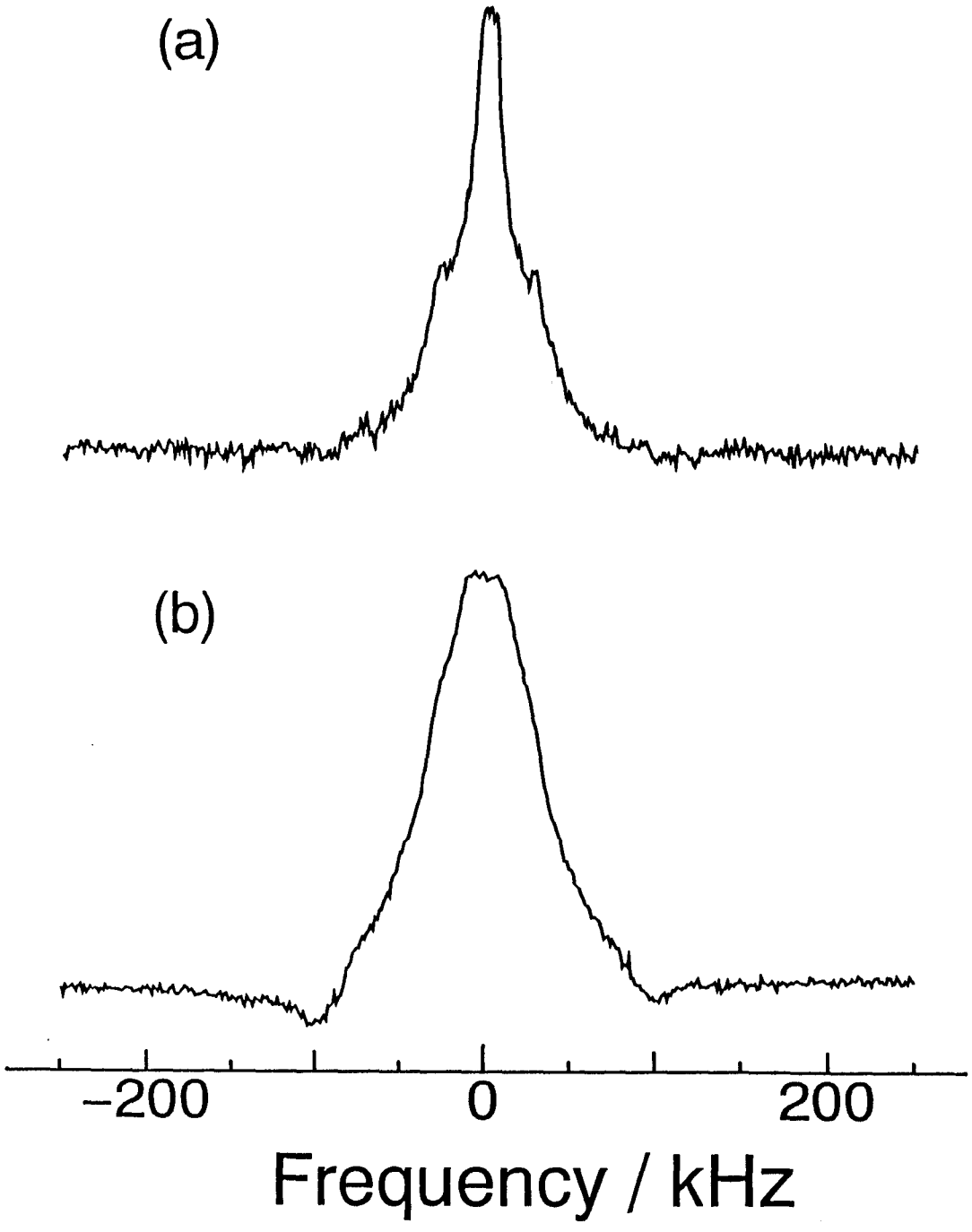

Fig. 2.9 The ^{2}H NMR spectra of $Na_3PMo_{12}O_{40} \cdot 6D_2O$ at (a) 286 K and (b) 180 K.

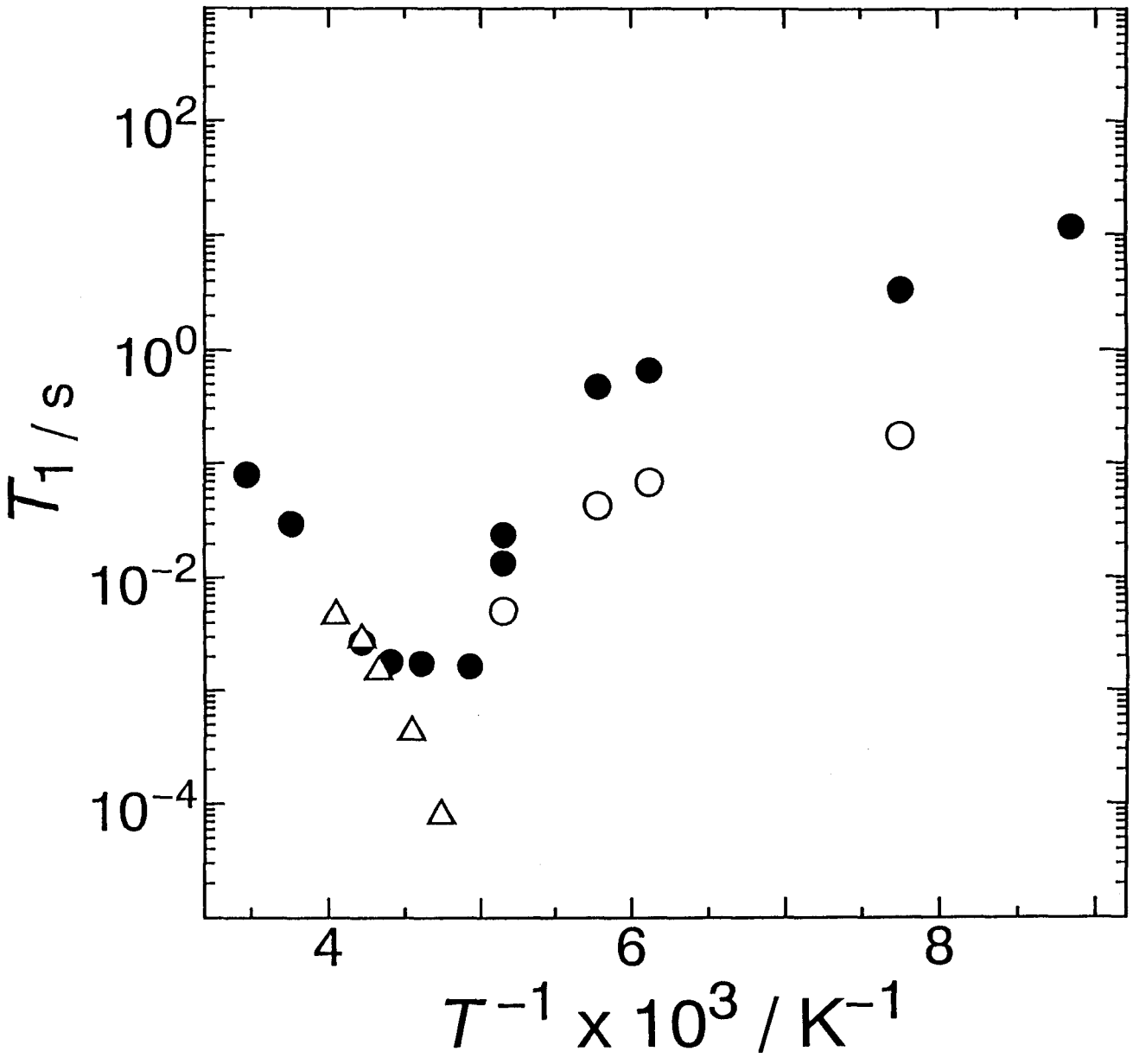

Fig. 2.10 The temperature dependence of the ^{2}H T_1 (the circles) and the T_2^* (the triangles) of $Na_3PMo_{12}O_{40} \cdot 20D_2O$ at 30.72 MHz. The T_1 is separated into two components below 200 K. The short component (open circle) corresponds to the central peak in the ^{2}H NMR spectrum and long one (closed circle) the outer.

so the T_1 could be separated into two components; the long T_1 corresponds to the outer component and the short one to the central component of the spectrum. T_2^* was estimated using the relation,

$$\Delta\nu = \frac{1}{\sqrt{2\pi}T_2^*},$$

where $\Delta\nu$ is the FWHM of the Lorentzian peak above 200 K. T_1 and T_2^* coincided with each other above 230 K.

2.2.4 ^{23}Na NMR

The temperature dependence of the ^{23}Na NMR spectrum and the T_1 at 52.94 MHz in the 29-hydrate are shown in Figs. 2.11 and 2.12, respectively. ^{23}Na NMR spectrum consists of a sharp peak at room temperature. Below 190 K the magnetization recovery became non-exponential and the maximum intensity of FID was observed at half the original 90° pulse length. The typical recovery curve of the ^{23}Na magnetization below 190 K are shown in Fig.2.13. Furthermore the line broadened suddenly at 190 K on cooling. These facts suggest that the ^{23}Na nuclear quadrupole coupling constant is nearly zero above 190 K whereas it assumes a finite value at lower temperatures.

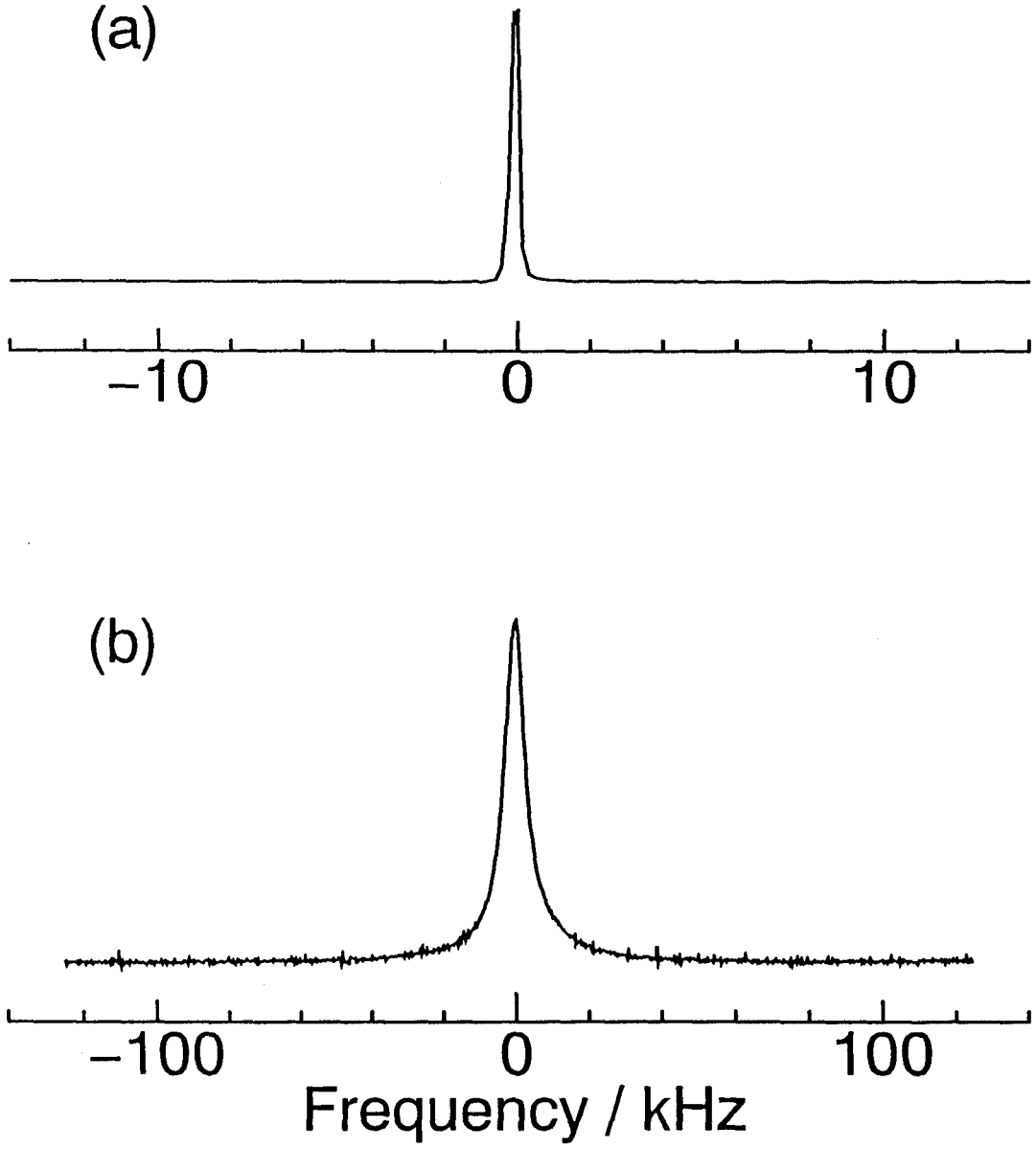

Fig. 2.11 ^{23}Na NMR spectrum of $Na_3PMo_{12}O_{40} \cdot 29H_2O$ at (a) room temperature and (b) 140 K.

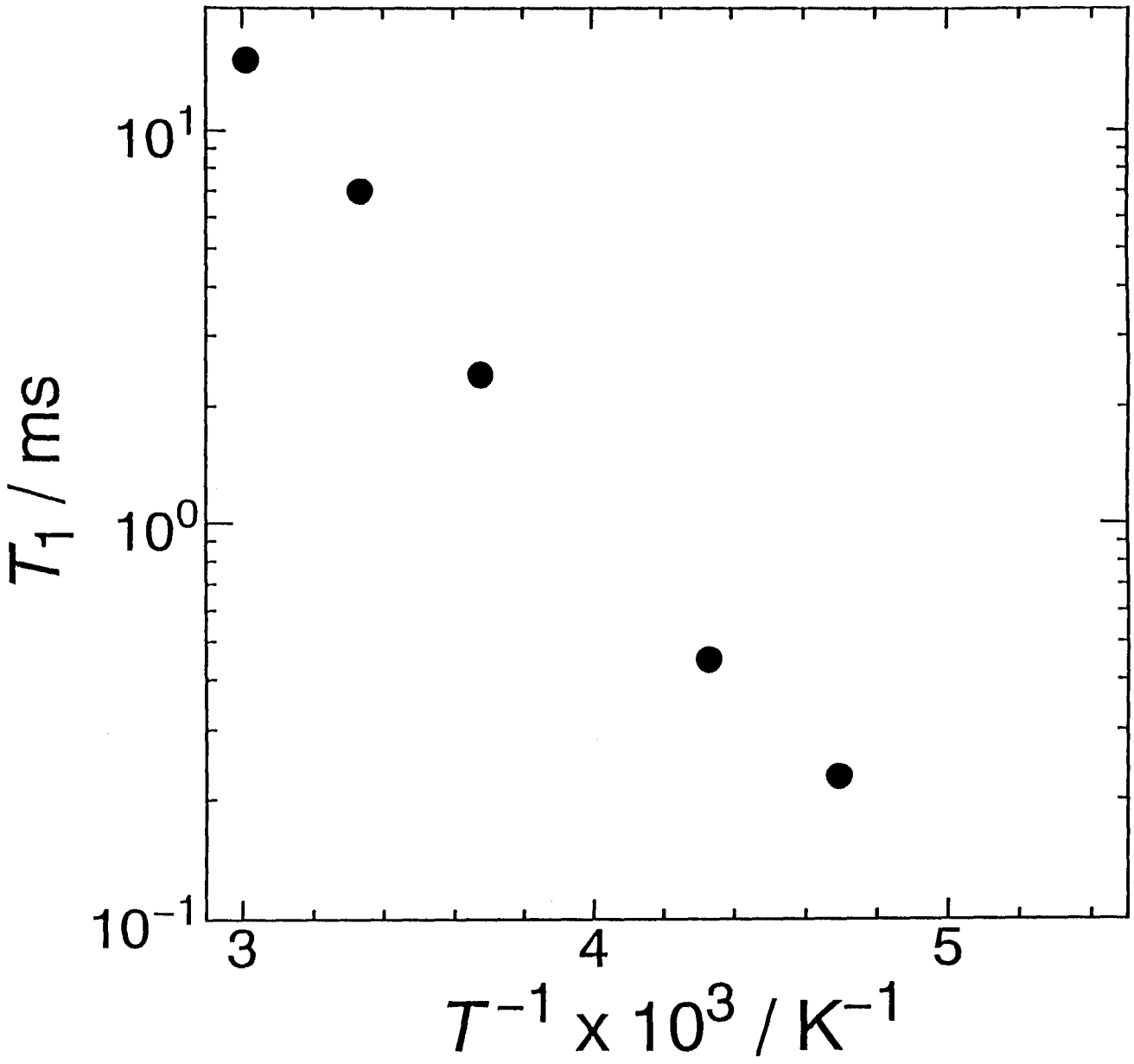

Fig. 2.12 The temperature dependence of the ^{23}Na T_1 of $Na_3PMo_{12}O_{40} \cdot 29H_2O$ at 52.94 MHz. The recovery of the magnetization was heavily non-exponential and the T_1 could not be determined below 200 K . This is characteristic of the spin $I > 1$ nuclei with non-zero quadrupole coupling.

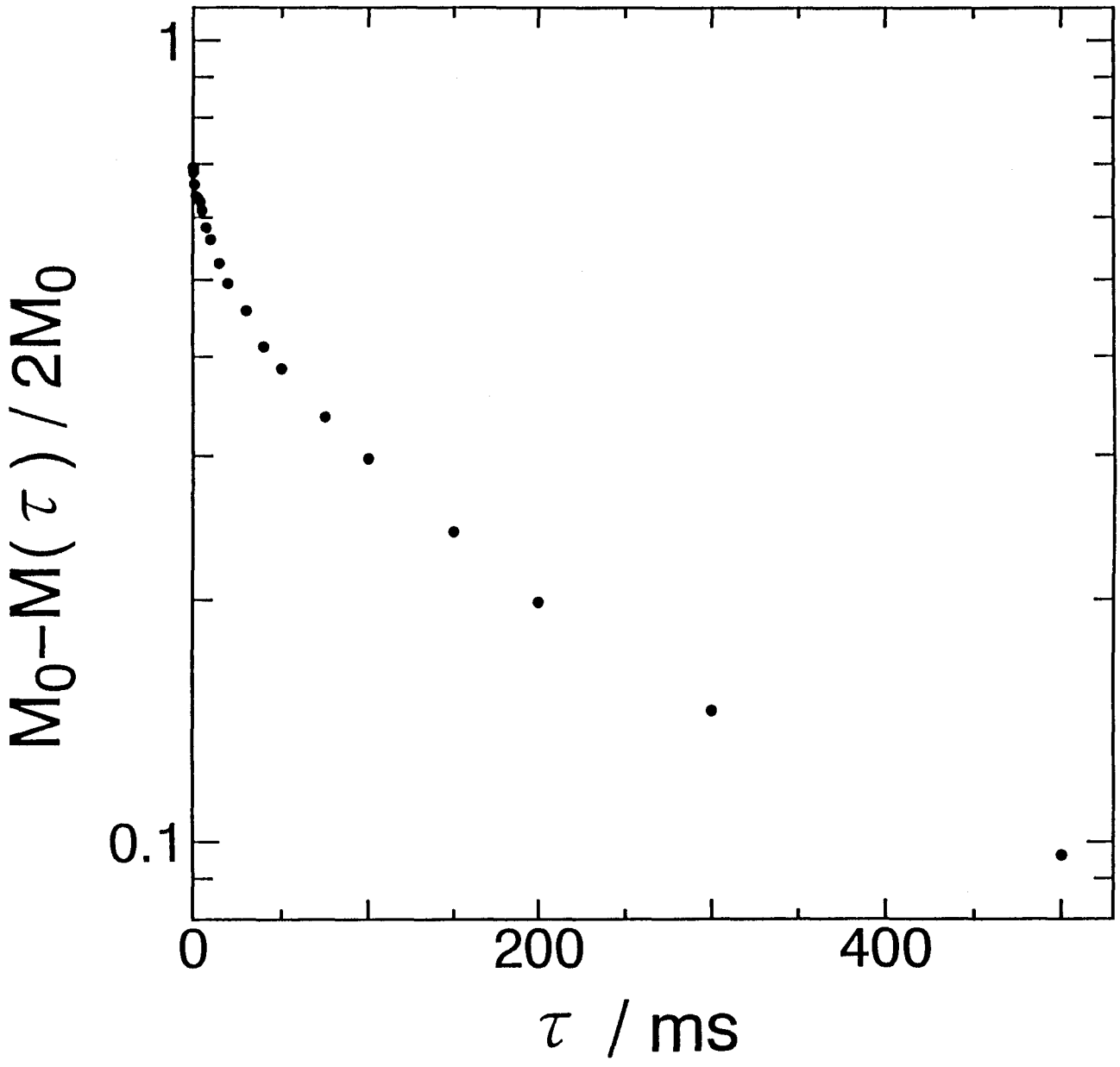

Fig. 2.13 The typical recovery curve of the ^{23}Na magnetization below 200K; this data was accumulated at 147 K.

2.3 Discussion

The NMR line shapes of the ^{1}H and ^{2}H are generally governed by the nuclear magnetic dipole-dipole interaction and the electric quadrupole interaction, respectively. These interactions are modulated by molecular motions. Thus the analysis of the individual line shape brings about the information on the type and the rate of the motion of the water molecules in present material.

First we consider the ^{1}H line shape of a single water molecule which undergoes some particular type of motion. The dipole-dipole interaction between the protons in a H_2O causes the splitting of the resonance line by an amount [3a],

$$\delta\nu_{\mathrm{H-H}} = \frac{3}{2}\frac{\gamma h}{r^3}(3\cos^2\theta - 1),$$

where γ is the gyromagnetic ratio of the proton, r the interproton distance, and θ the angle between the static magnetic field and the vector which connects the two protons. In a system consisting of randomly oriented static molecules, *i.e.*, in a powdered specimen, the splitting is averaged over the spatial distribution of the ^{1}H $-^1$ H vectors and then the spectrum gives a Pake pattern (Fig. 2.14a). Actually, the spectrum is broadened by the intermolecular dipole-dipole interaction which must be large in the case of the 29-hydrate. The theoretical line shape for the rigid water molecules with the Gaussian broadening of 10.6 kHz is also shown in Fig. 2.14d. Fig. 2.14b and c are the line shapes for H_2O molecules undergoing fast rotation around the molecular C_2-axis and fast isotropic rotation, respectively.

The spectrum of the 29-hydrate between 109 K and 209 K can be represented by the

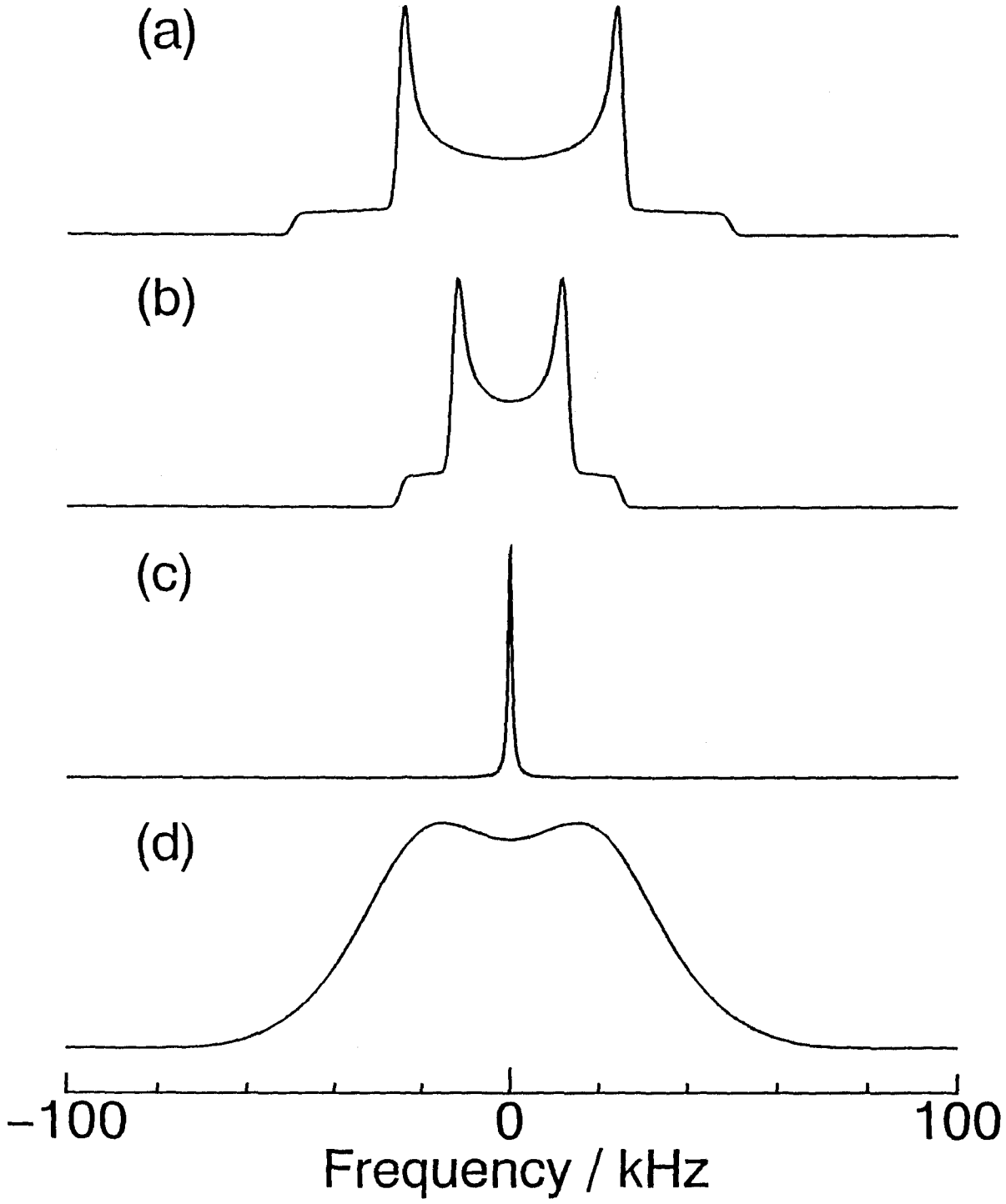

Fig. 2.14 The simulated ^{1}H NMR line shape for H_2O molecules in some particular cases: (a) randomly oriented static molecules, (b) the molecules undergoing fast rotation about the molecular C_2 axis, (c) the molecules undergoing isotropic rotation, and (d) the same as (a) with 10.6 kHz Gaussian broadening. See text for details.

superposition of a Pake pattern with the Gaussian broadening and a single Lorentzian line; the full width is 112 kHz and the Gaussian broadening is 9.8 kHz at 109 K. The theoretical line shapes which give best fit to the experimental line shapes at individual temperatures are shown in Fig.2.15-22 and the fitting parameters are listed in Table 2.1. The outer component is attributed to the static water molecules in which the interproton distance is 1.47Å, and the central component to the molecules undergoing the isotropic rotation. However the possibility that the apparently "static" molecules undergo the 180° flip can not be ruled out at present because we can not distinguish a rigid and a 180°-flipping molecule by the ^{1}H NMR spectrum. Later it will be shown that these two states can be distinguished by the ^{2}H line shape analysis.

The spectrum of the 29-hydrate at room temperature consists of an extremely narrow peak which corresponds to the case where the intermolecular dipole interaction with the strength of 6.4 kHz at 150 K is quenched. This fact indicates that the water molecules undergo not only the isotropic rotation but fast translational diffusion; this means that the water is in the *pseudoliquid* state as suggested in ref. 1. The spectrum changes from the single peak to one with two components at about 190 K on cooling. This temperature coincides with the transition temperature from Phase II to Phase III. It can be defined as the "freezing" temperature of the pseudoliquid water.

The temperature dependence of the line width of the simulated central component is shown in Fig. 2.23. The line width increases linearly with decreasing in temperature from 209 K to 171 K. This line broadening indicates that the rate of the water motion

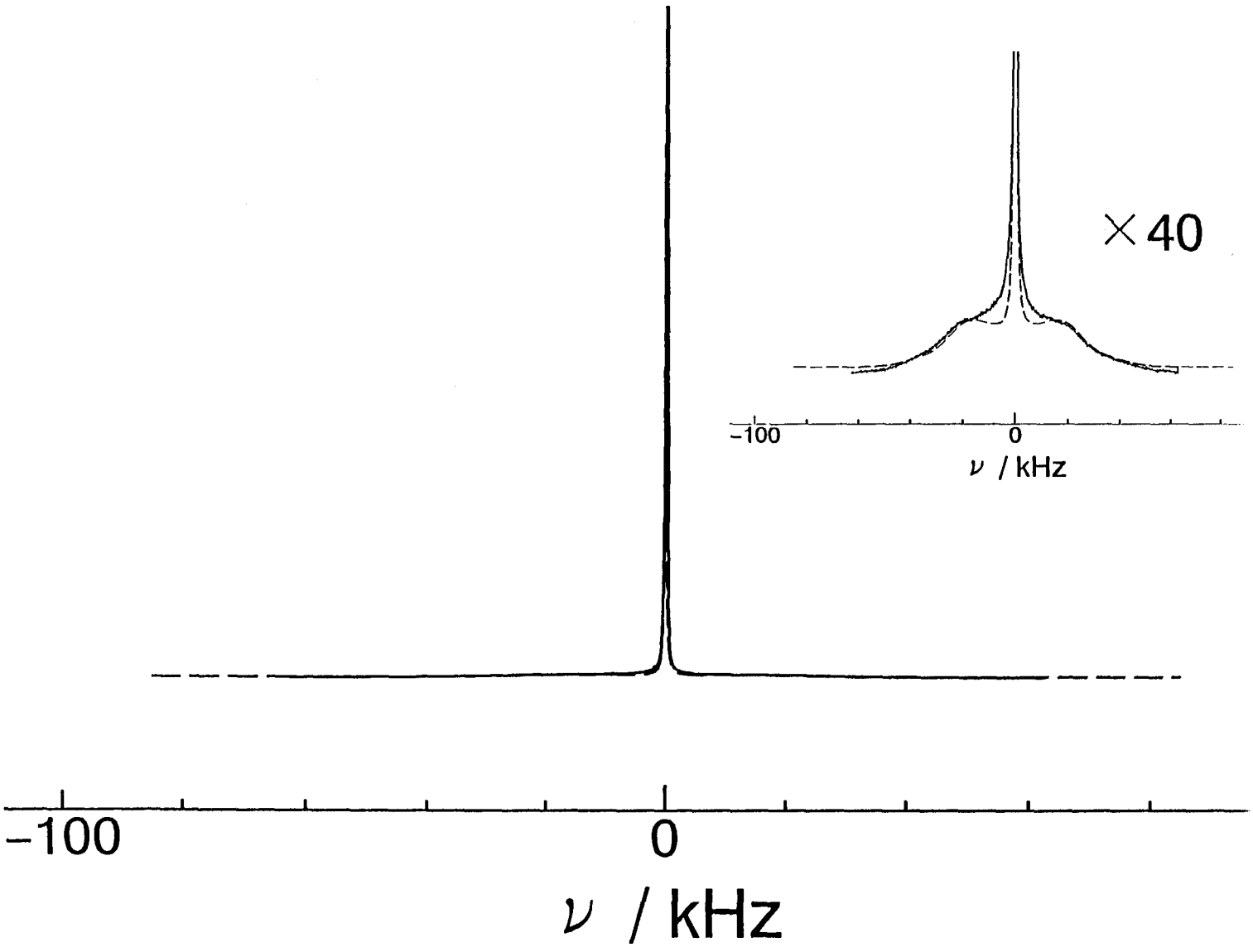

Fig. 2.15 Experimental and theoretical ^{1}H spectrum: The solid line is the observed spectrum at 209 K and the broken line represents the best fit; the fitting parameters are given in Table 2.1.

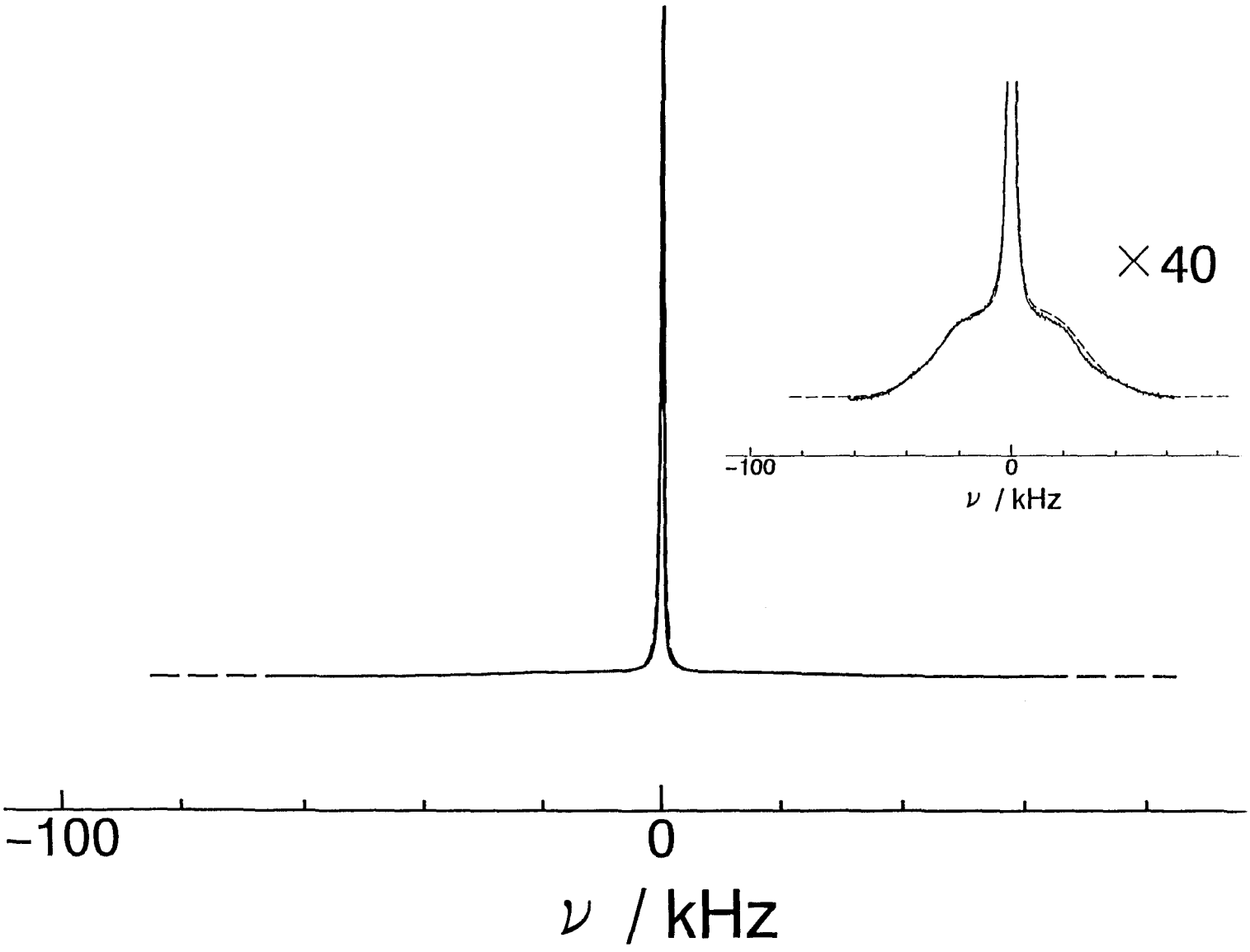

Fig. 2.16 Experimental and theoretical ^{1}H spectrum: The solid line is the observed spectrum at 199 K and the broken line represents the best fit; the fitting parameters are given in Table 2.1.

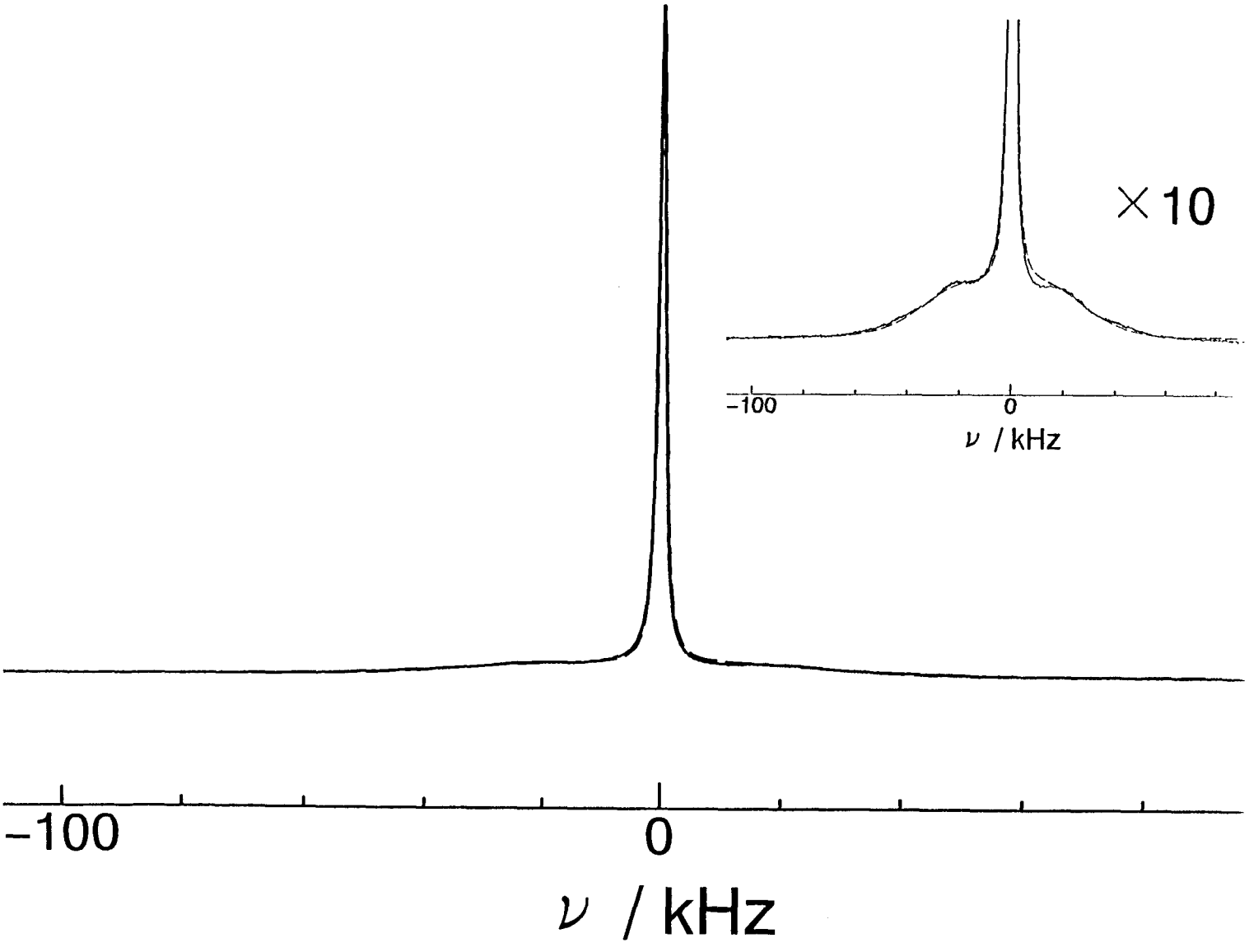

Fig. 2.17 Experimental and theoretical ^{1}H spectrum: The solid line is the observed spectrum at 189 K and the broken line represents the best fit; the fitting parameters are given in Table 2.1.

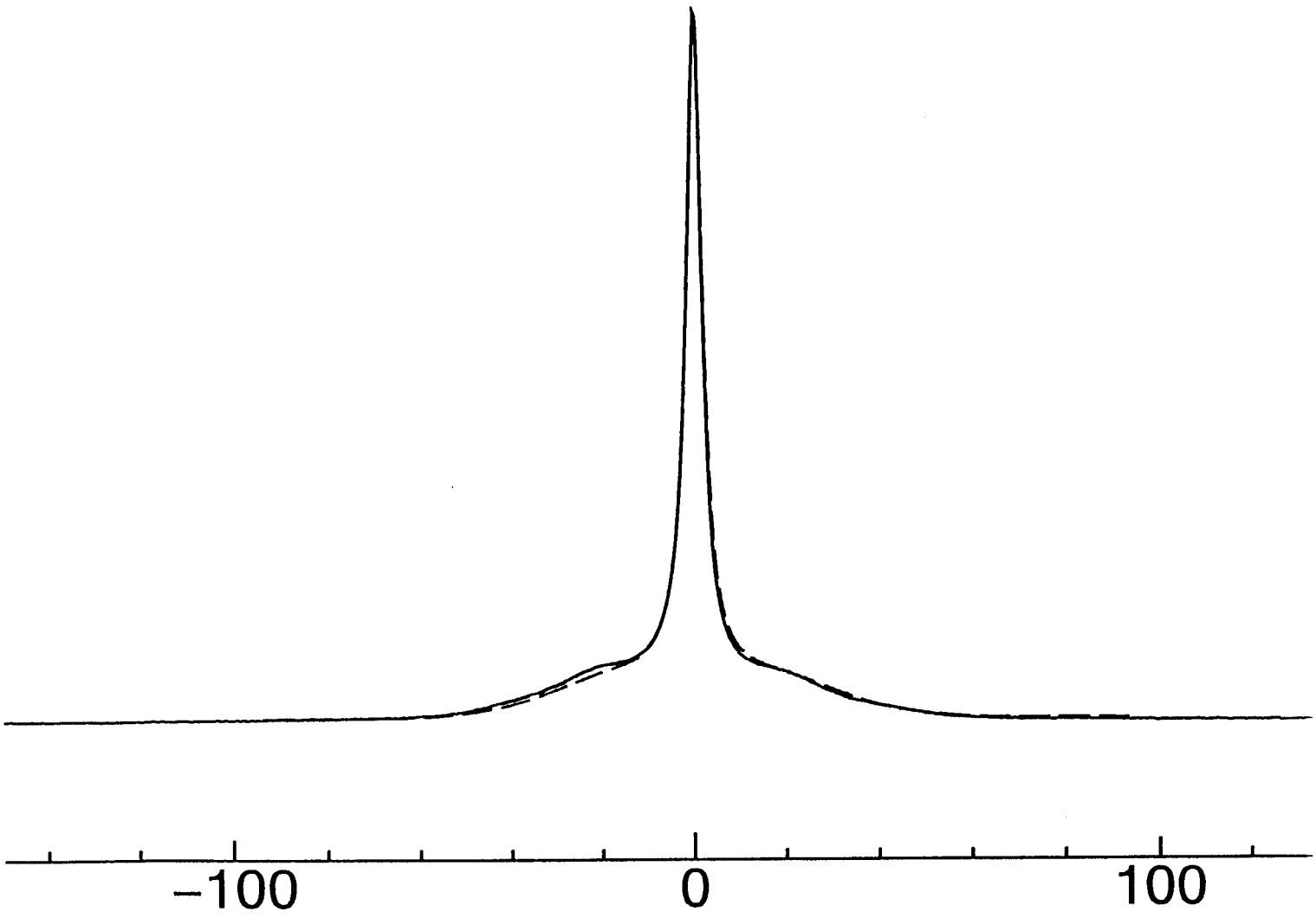

Fig. 2.18 Experimental and theoretical ^{1}H spectrum: The solid line is the observed spectrum at 180 K and the broken line represents the best fit; the fitting parameters are given in Table 2.1.

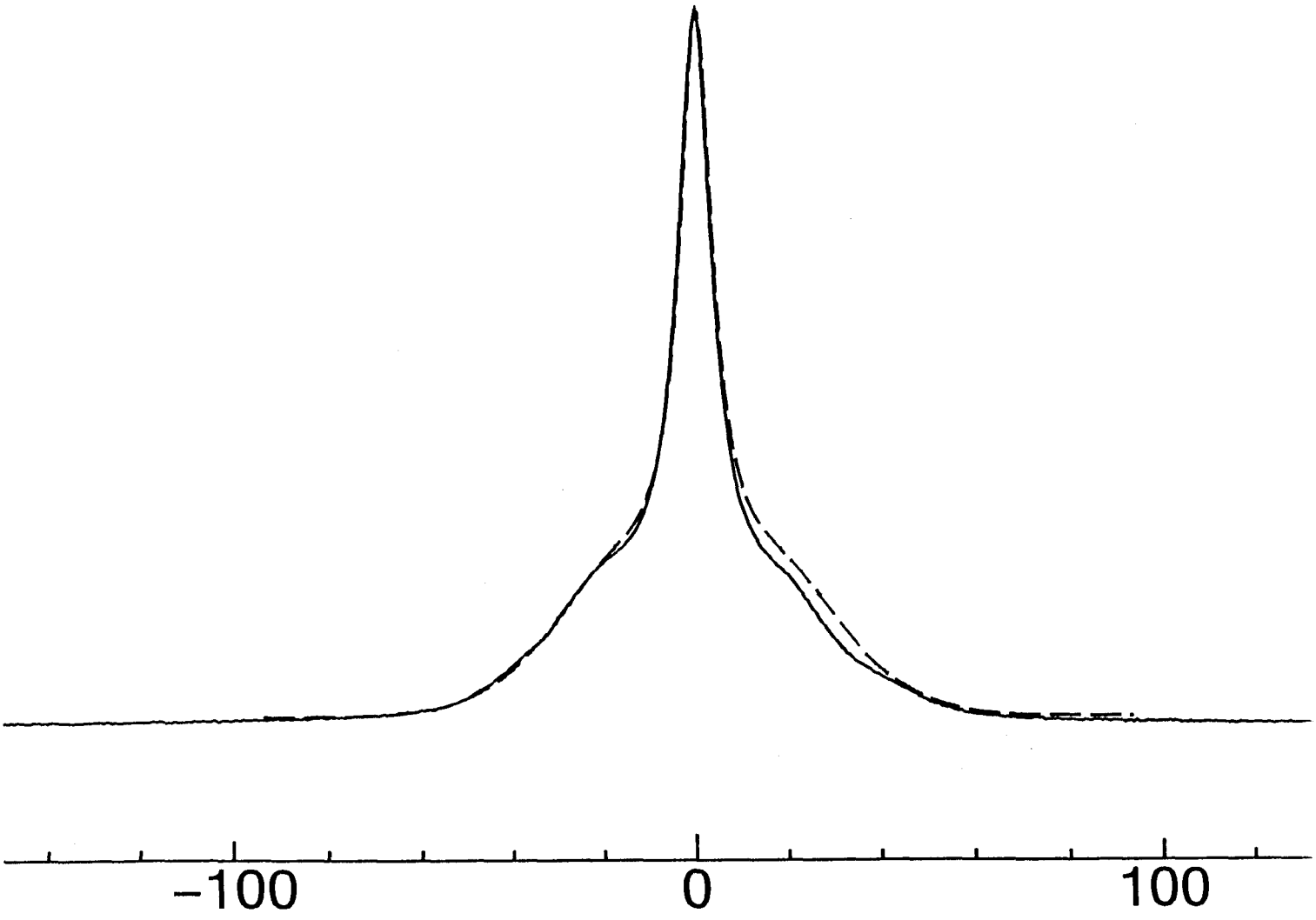

Fig. 2.19 Experimental and theoretical ^1H spectrum: The solid line is the observed spectrum at 171 K and the broken line represents the best fit; the fitting parameters are given in Table 2.1.

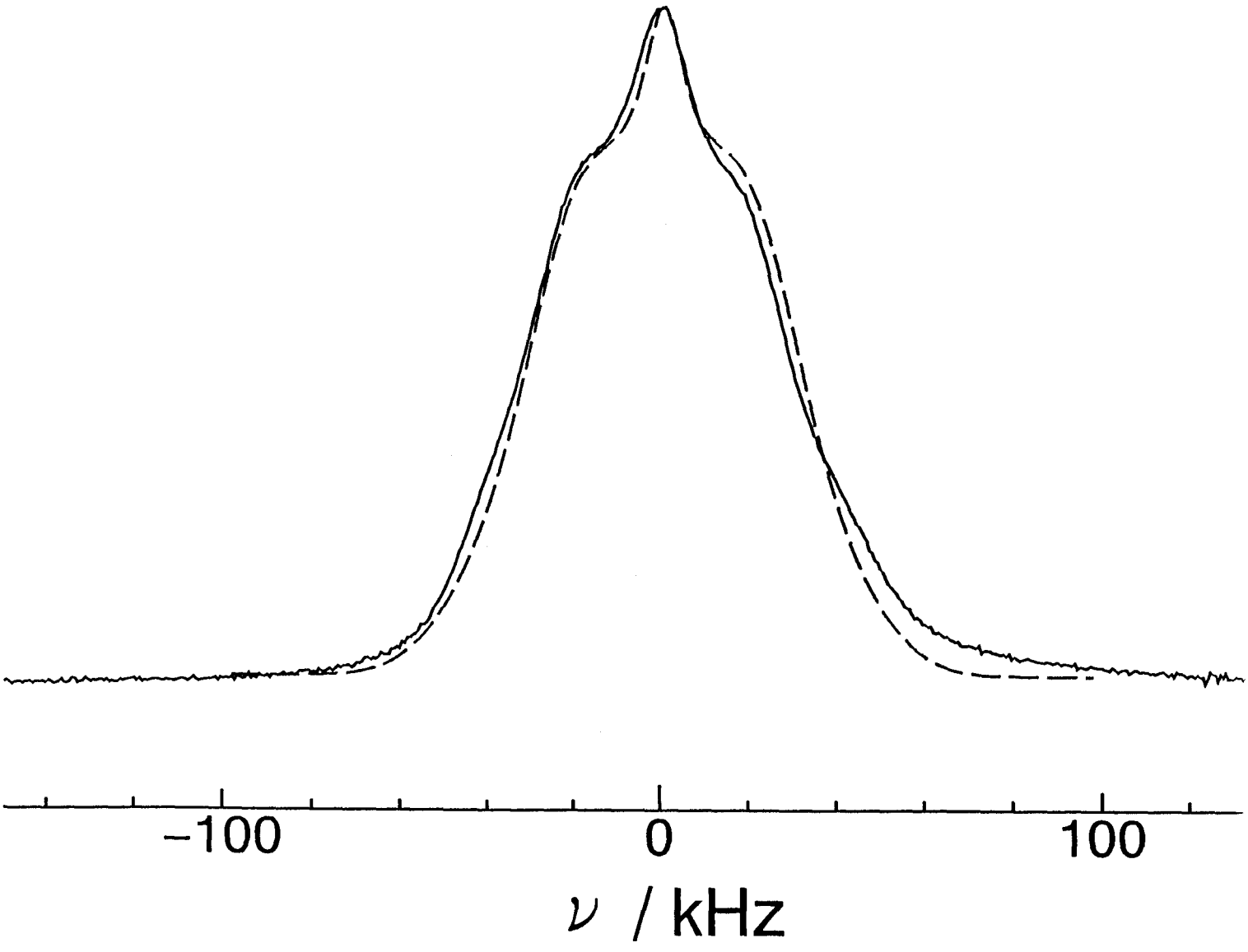

Fig. 2.20 Experimental and theoretical ^{1}H spectrum: The solid line is the observed spectrum at 157 K and the broken line represents the best fit; the fitting parameters are given in Table 2.1.

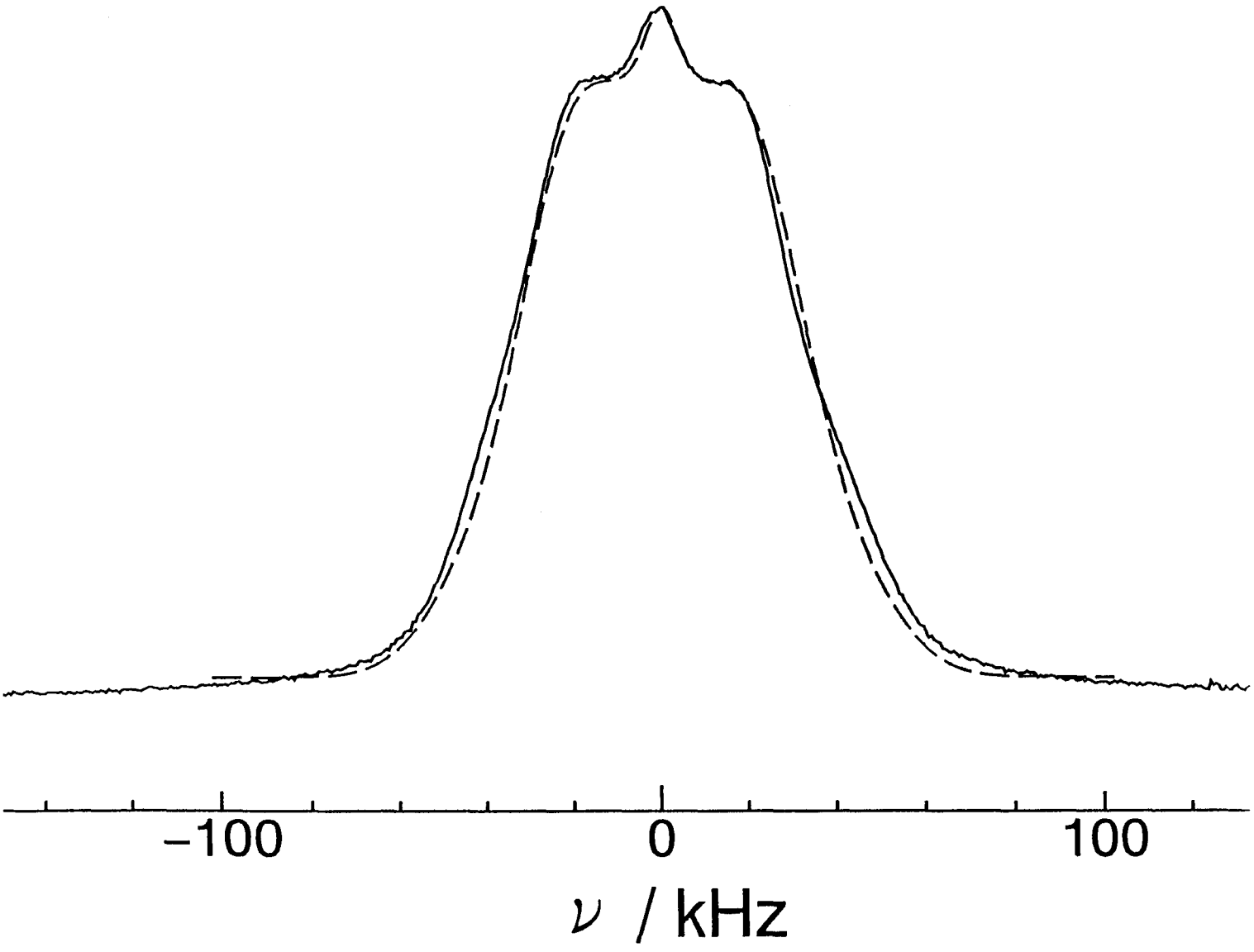

Fig. 2.21 Experimental and theoretical ^{1}H spectrum: The solid line is the observed spectrum at 150 K and the broken line represents the best fit; the fitting parameters are given in Table 2.1.

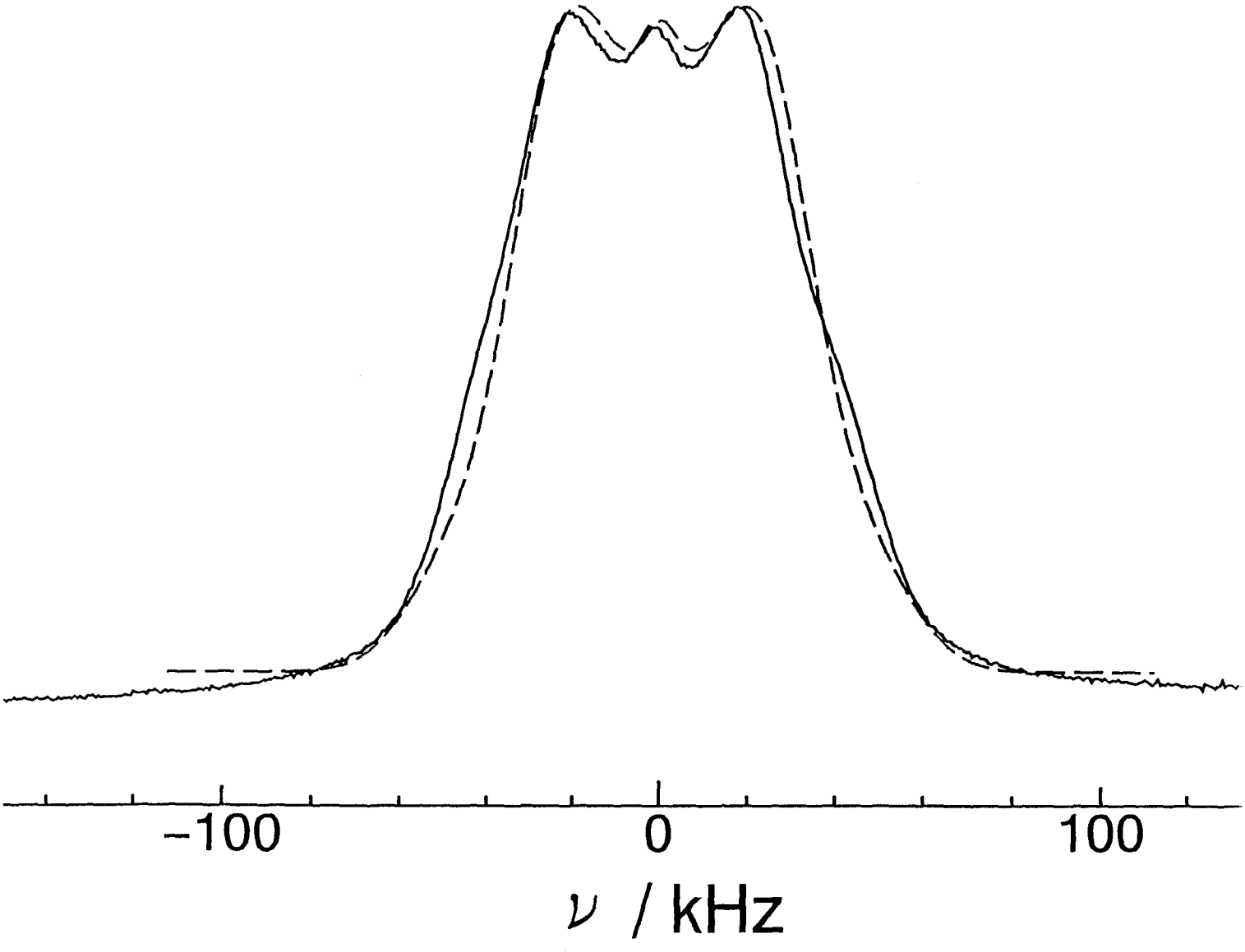

Fig. 2.22 Experimental and theoretical ^{1}H spectrum: The solid line is the observed spectrum at 109 K and the broken line represents the best fit; the fitting parameters are given in Table 2.1.

T / K	outer Pake pattern			central lorentzian	
	$\Delta\nu$ / kHz	broadning / kHz	ratio	FWHM / kHz	ratio
109	112.4	9.8	0.966	6.39	0.034
150	102.2	10.6	0.940	6.39	0.060
157	97.9	10.6	0.898	4.26	0.102
171	93.7	10.6	0.573	4.26	0.427
180	93.7	10.6	0.403	2.13	0.597
189	93.7	10.6	0.375	0.68	0.625
199	85.2	9.4	0.322	0.30	0.678
209	85.2	6.4	0.330	0.15	0.670

Table 2.1 The fitting parameters for the ^{1}H line shape of $Na_3PMo_{12}O_{40} \cdot 29H_2O$. $\Delta\nu$ is the peak-topeak splitting of the Pake pattern.

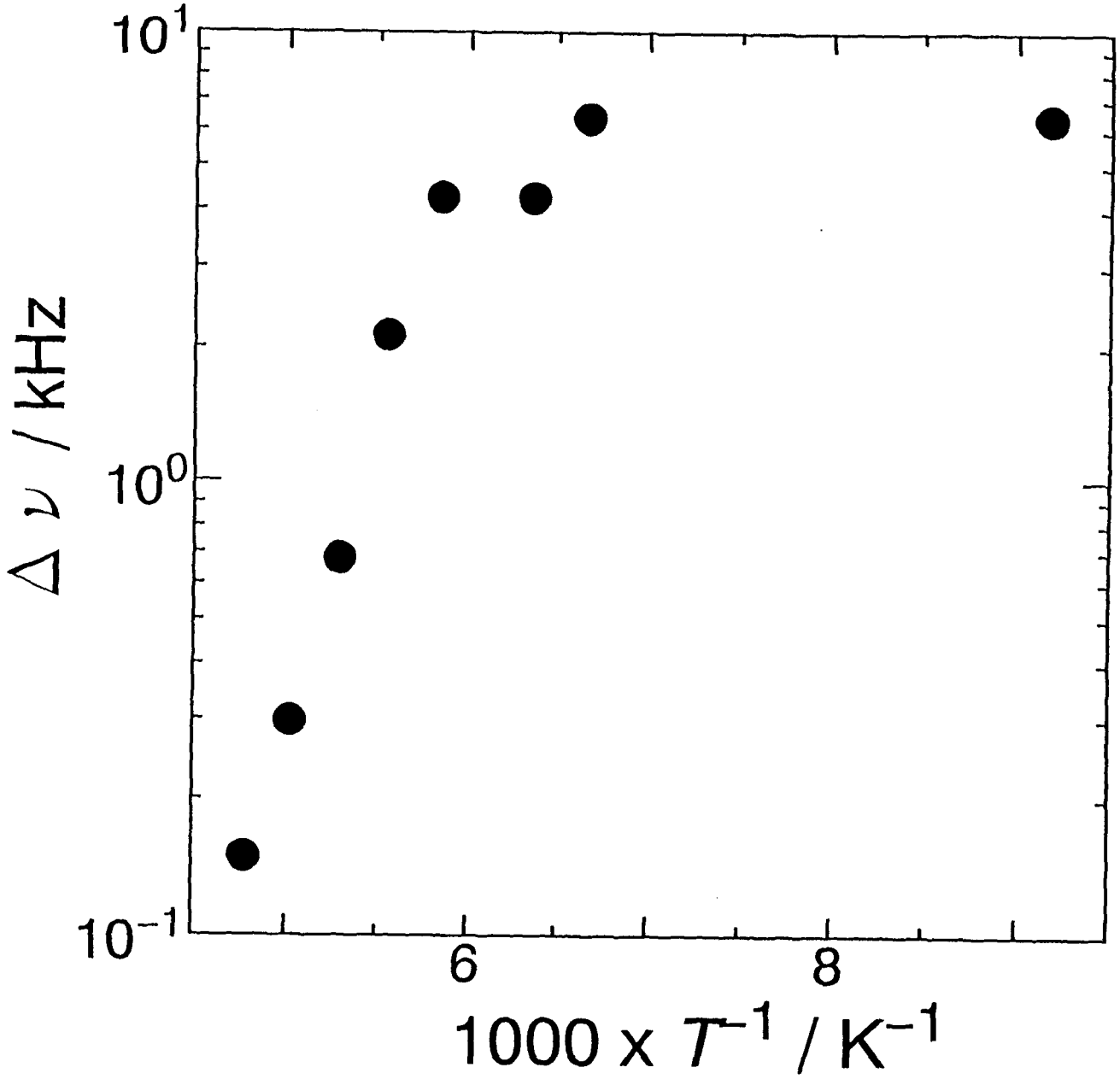

Fig. 2.23 The plott of the theoretical line width of the central component which are listed in Table 2.1 versus temperature.

decreases stochastically on cooling. The line width $\Delta\nu$ can be related to the correlation time for the motions as [3a]

$$\Delta\nu \simeq 1/T_2 = (\delta\omega_D)^2\tau_c$$

where $\delta\omega_D$ is the spread in frequency corresponding to the spread of dipolar local field. Assuming the Arhenius activation process,

$$\tau_c = \tau_0 e^{-E_a/RT},$$

the activation energy for the motion of water molecule is estimated to be 26.5 kJ mol^{-1}. At lower temperatures below 171 K it seems that the line width remains constant, but since the ratio of the central component is extremely low and the fitting parameter for it is less reliable in these lowest temperature region. Two motional modes of H_2O molecule can be considered to govern the line width below 209 K; one is the isotropic rotation of the water molecule and the other the translational diffusion. Because the intramolecular dipolar interaction is averaged out and only the intermolecular dipolar width (6.4 kHz) remains at 171 K. The former motion do not give rise to further narrowing. Hence the mode which contribute to the narrowing above 171 K is assigned to the diffusion of H_2O molecules.

The proportion of the central component to the total intensity at each temperature was estimated by the above simulation of the line shape and is plotted in Fig. 2.24. The ratio changes continuously with temperature. It is approximately constant in the region between 180 K and 200 K and below 140 K. The plot implies that there are more than two kinds of water molecules in the crystal; one is easy to freeze and quite mobile. Its fraction

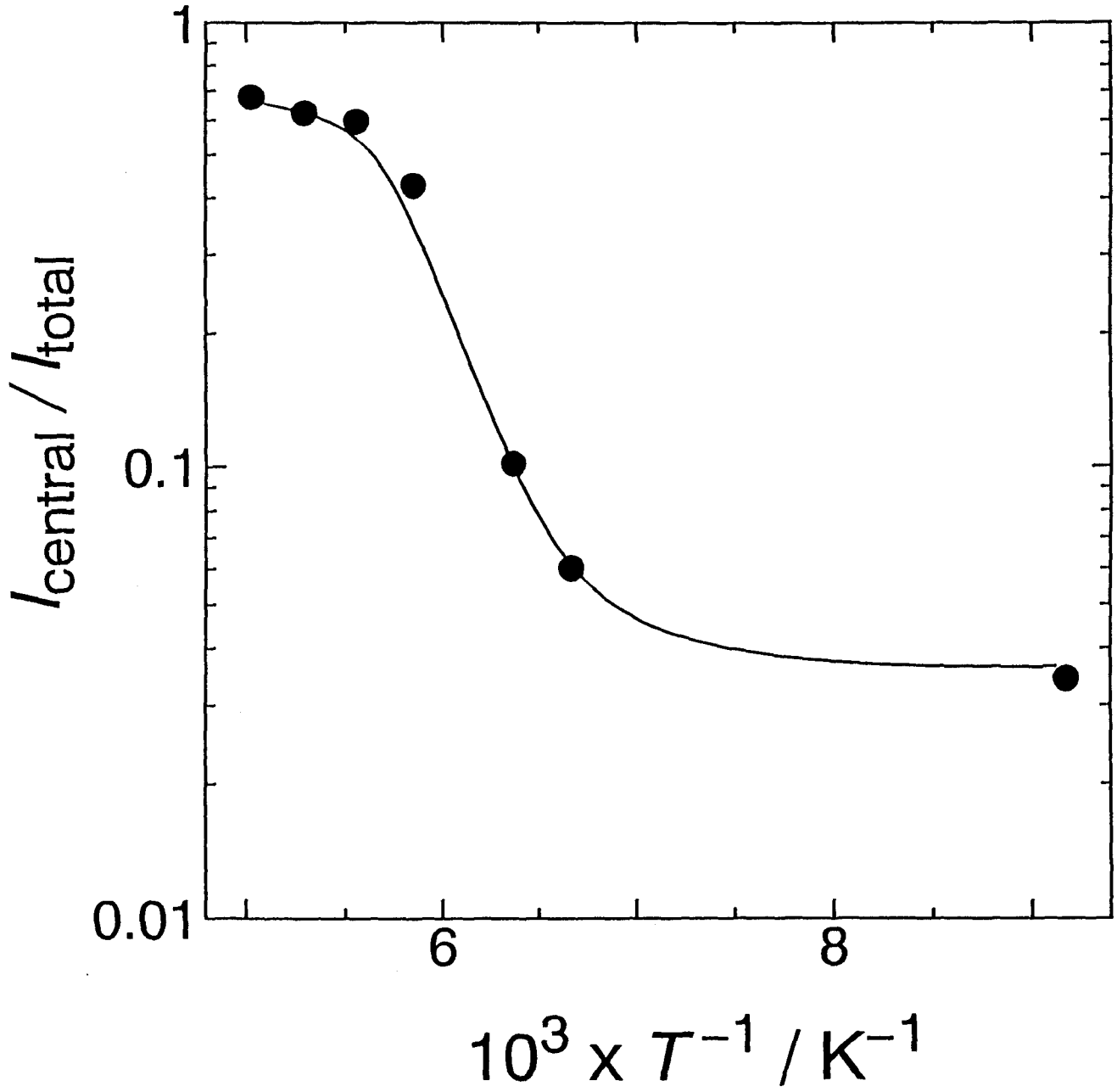

Fig. 2.24 The temperature dependence of the intensity ratio of the narrow component to the total intensity of ^1H NMR spectrum of $Na_3PMo_{12}O_{40} \cdot 29H_2O$ below 200 K. The solid line is the guide line for the eyes.

is about 70% above 180 K, decreases sharply at low temperatures to a negligible amount below 140 K. Another kind is relatively rigid, the fraction of which increases on cooling. Providing that the gross structure of the trisodium dodecamolybdophosphate is analogous to that of the dodecatungustophosphoric acid [4], we can distinguish various different sites for the water molecules, *i.e.*, sites at close proximity of the Na^+ ion, interstitial sites between anions, and intermediate sites between these sites. However, we can not distinguish which one among these sites is the mobile site in the present stage. This point will be discussed later.

In the case of the hexahydrate the line shape varies continuously with temperature and it is still significantly broad even at room temperature, implying that the highly mobile, pseudoliquid water molecules have been lost in the material. The motional state of the water molecule will be discussed later together with the analysis of ^2H resonance.

Next we will examine the ^2H NMR spectrum. The line shape of the ^2H is governed mainly by the nuclear quadrupole interaction and the magnitude of the quadrupole splitting is given in ref. 3b as follows:

$$\delta\nu = \frac{3}{4}\frac{e^2Qq}{h}(3\cos^2\beta - 1 - \eta\sin^2\beta\cos\alpha),$$

where $\frac{e^2Qq}{h}$ is the quadrupole coupling constant and (α, β, γ) the Euler angles to convert the coordinate system from the laboratory fixed frame to the principal axis system of the electric field gradient (EFG) tensor. η is the asymmetric parameter for the EFG which is

defined as

$$\eta = (V_{xx} - V_{yy})/V_{zz}.$$

by using the components $V_{xx} = \dfrac{\partial V}{\partial x^2}$, *etc.*, of the EFG tensor, where V is the electrostatic potential at the probing nucleus. In a D_2O molecule the direction of the principal z-axis coincides with the O-D bond direction and η can be assumed to zero. In this case the EFG tensor can be written in a very simple form,

$$V = \begin{pmatrix} V_{xx} & 0 & 0 \\ 0 & V_{yy} & 0 \\ 0 & 0 & V_{zz} \end{pmatrix} = \begin{pmatrix} -\frac{eq}{2} & 0 & 0 \\ 0 & -\frac{eq}{2} & 0 \\ 0 & 0 & eq \end{pmatrix}.$$

Then the quadrupole-perturbed line shape for the randomly oriented rigid D_2O molecules is calculated as shown in Fig. 2.26a. In the case that the molecule undergoes some rapid motion the EFG tensor is averaged in the characteristic manner to the motional mode. For example, when the molecule undergoes fast 180° flipping about the molecular two-fold axis, the EFG tensor between the directions, z1 and z2, is averaged as shown in Fig. 2.25; the averaged EFG tensor is then represented in the principal axis system $Oxyz$ by

$$\begin{aligned} V^{\text{avg}} &= \begin{pmatrix} V_{yy} & 0 & 0 \\ 0 & V_{xx}\cos^2\theta + V_{zz}\sin^2\theta & 0 \\ 0 & 0 & V_{yy}\sin^2\theta + V_{zz}\cos^2\theta \end{pmatrix} \\ &= -\frac{eq}{2}\begin{pmatrix} 1 & 0 & 0 \\ 0 & \cos^2\theta - 2\sin^2\theta & 0 \\ 0 & 0 & \sin^2\theta - 2\cos^2\theta \end{pmatrix}, \end{aligned}$$

where θ is the half of the bond angle, ∠D-O-D and is 52.26° for H_2O. Then the new z-axis of the EFG tensor comes on the x-axis of the original EFG tensor, and so the quadrupole coupling constant becomes $\frac{1}{2}\frac{e^2Qq}{h}$ the asymmetry parameter is is changed to $\eta = 0.75$. Fig. 2.26b-d are the simulated powder line shapes for a D_2O molecule when it undergoes

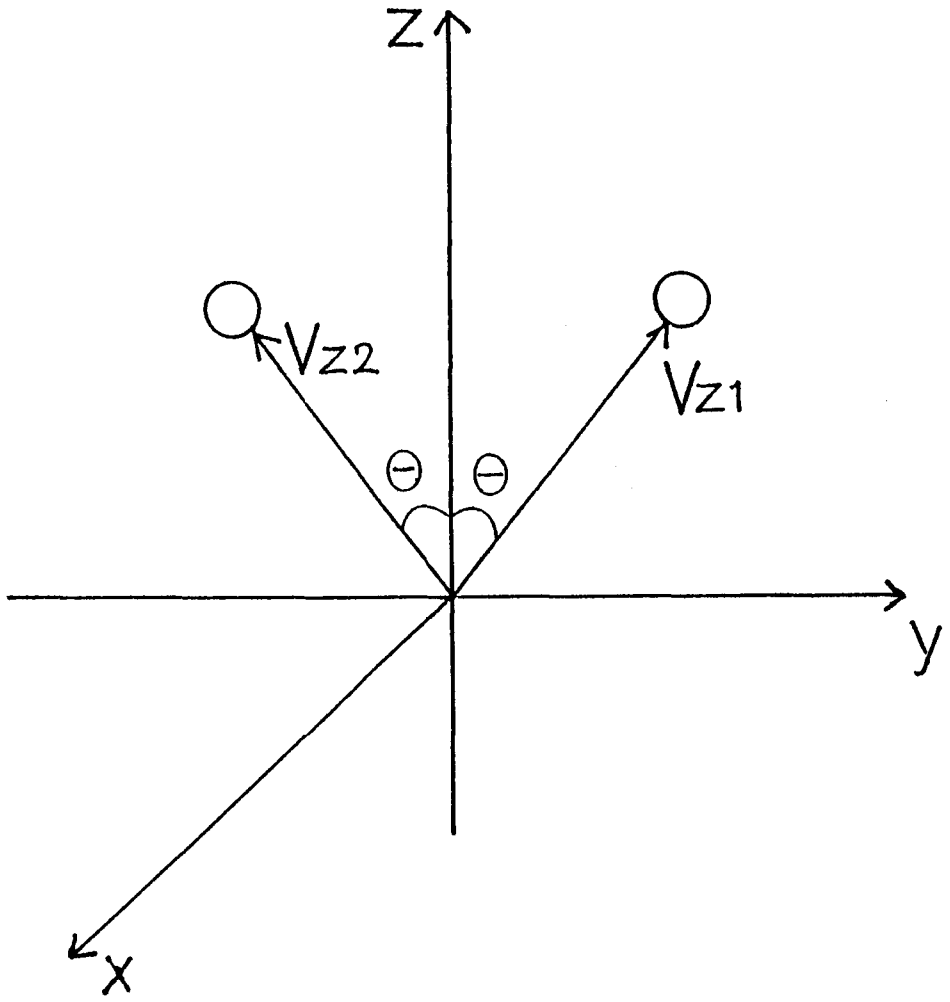

Fig. 2.25 The principal axis system *Oxyz* for a D_2O molecule undergoing fast 180° flipping motion .

a various kind of fast motion. The experimental line shape of the outer component of the 20-hydrate below 200 K in Fig. 2.8c fits the theoretical one for rigid molecule with $\frac{e^2Qq}{h} \sim 220$ kHz; this value agrees with the reported value, 216.4 kHz, for D_2O ice [5]. At room temperature the spectrum shows a sharp peak, indicating that the D_2O molecules are in the pseudoliquid phase and undergo rapid isotropic rotation in the 20-hydrate. The central component below 200 K has a structure and the most part corresponds to the molecules undergoing the 180°-flipping about the C_2 axis, but is superimposed by some other fast motion.

From these observations we can model a structure of waters in the crystal lattice: In the water-saturated crystals the most fraction of water molecules come together to form a pseudoliquid phase at room temperature. This phase freezes cooperatively below *ca.* 200 K to form a rigid, ice-like hydrogen bonded structure. In the hexahydrate, on the other hand, the water molecules are bounded probably at the active sites of the host lattice. They are isolated from each other and do not experience any cooperative force by other water molecules. The motion is governed only by neighboring ions and so depends very weakly on temperature.

We will next analyze the ^1H T_1 of the 29-hydrate in Fig. 2.7. It assumes the minimum value of 11 ms at 207 K due obviously, from the spectrum (Fig. 2.5) discussed in a previous section, to the isotropic rotation of the water molecules. In the case where the molecular isotropic rotation governs the dipolar relaxation of the ^1H T_1 is given by [3a]

$$T_1^{-1} = A\{\frac{\tau_c}{1+\omega^2\tau_c^2} + \frac{4\tau_c}{1+4\omega^2\tau_c^2}\},$$

$$A = \frac{3}{10}\frac{\gamma^4\hbar^2}{r^6},$$

where ω is the proton Larmor frequency, τ_c the correlation time of the motion, and r the interproton distance. Using $r = 1.47$ Å the theoretical minimum value of the T_1 at $\frac{\omega}{2\pi} = 18.1$ MHz is 7.6 ms. The experimental value 11 ms is larger than this value. This fact suggests that some fraction of structural water molecules are static and do not contribute to the relaxation.

The fitting of the above equation to the experimental T_1 in Fig. 2.7 leads to activation energy for the isotropic rotation of 25.9 kJ mol^{-1} between 172 K and 240 K. The pre-exponential factor τ_0 was calculated to be 0.12 s using the relation $\omega\tau_c \simeq 0.616$ at the minimum. The two transitions, Phases II $\leftrightarrow$ III and III $\leftrightarrow$ IV, exist in this temperature region but do not affect the water motion.

It is interesting to see that the E_a for the isotropic rotation agrees with the value estimated from the temperature dependence of the line width of the central component which was assigned to the activation energy for the translational diffusion; this means that rapid rotation ($\sim 10^{-8}$ Hz) and slow diffusion take place with almost the same activation energy. In the Phase I above 270 K the value of the activation energy is reduced to 12.4 kJ mol^{-1}. On the other hand a constant value 21.3 kJ mol^{-1} was obtained by ^{23}Na T_1 between 210 K and 330 K (Fig. 2.12). This value agrees fairly well with the E_a for the isotropic rotation of water molecule determined above by the ^{1}H T_1 measurement below 240 K. Therefore the mode of the molecular motion which governs the ^{1}H T_1 in Phase I above 270 K is different from the isotropic rotation; comparing the activation energy,

12.4 kJ mol^{-1} with 15.4 kJ mol^{-1} [6] for the translational diffusion of water molecule in bulk water, it may be attributed to the translational diffusion of water molecules which are free from the hydrated spherical cation in the pseudoliquid phase. This sort of water was called before "intermediate water". It is interesting to see that the activation energy for the diffusion is lower than that for the molecular isotropic rotation in the pseudoliquid water.

The relaxation of ^{2}H is governed by the nuclear quadrupole interaction. The quadrupolar spin-lattice relaxation is mostly caused by molecular reorientation or rotation. The translational motion does not generally contribute it. The relaxation rate, $\frac{1}{T_1}$, for spin $I = 1$ nucleus can be represented by the same formulae as for the dipole-dipole relaxation but the prefactor A is given by [3b],

$$A = \frac{3}{80}(1 + \frac{\eta^2}{3})(\frac{e^2Qq}{h})^2,$$

where η is the asymmetric parameter of the electric field gradient. The minimum value of T_1 for the isotropic rotation of D_2O is predicted to be 1.6 ms at $\frac{\omega}{2\pi}$=30.7 MHz using the values $\frac{e^2Qq}{h}$=220 kHz and η=0. This agrees well with the experimental value, 1.6 ms at 200 K as can been seen Fig. 2.10. The value of the activation energy for the motion above 230 K, 41.8 kJ mol^{-1}, which is very large compared with the value 25.9 kJ mol^{-1} in 29-hydrate. This large difference in E_a can be interpreted by considering that the some of water molecules are bounded to Na^+ to form the hydrated sphere. In concentrated solution contains Na^+ such as NaOH the structure of the water around the cation is very similar to the hydrate water in crystal such as $Na_2SO_4 \cdot 10H_2O$[7]; the average O-Na^+ distance is

2.43 Å. The coordination number is different for various substances but generally equal to 5 or 6. The pseudoliquid water in 12-molybdophosphate crystal is the intermediate state between the concentrated solution and rigid crystal, thus it is considered that this value is also available for this case. Because moment of inertia of this hydrated cation becomes large by deuteration , about 1.07 times , the larger activation energy is necessary for $Na^+ \cdot xD_2O$ to cause the rotation if x is the same. In this case the difference of the activation energy is too large to attribute to the difference of moment of inertia, but the difference of hydration number is important factor: When 6 water hydrate to Na^+, there are scarcely interstitial water for deuterated 20hydrate.

The two components of the T_1 below 190 K have the same temperature dependence and give the activation energy of 16.5 kJ mol^{-1} below 170 K. This activation energy is attributed to the reorientation or 180°-flip of the D_2O molecule about its molecular C_2 axis by referring to the ^{2}H NMR spectrum.

Although it was pointed out before that the ^{1}H line shape measurement can not distinguish between the rigid (static) water molecule and the molecule undergoing 180°-flipping, ^{2}H resonance can distinguish 180°-flipping molecule from static one. It is likely that 180°-flipping occurs in 29-hydrate at room the lowest temperature.

In the case of deuterated hexahydrate the spectrum shows somewhat complicated spectrum even at room temperature (see Fig. 2.9a) analogous to the ^{1}H spectrum of hexahydrate. The spectrum changes continuously with temperature and it is likely to converge to the line shape when the water undergoes fast rotation around molecular two-fold axis

(Fig. 2.26c). At low temperature the spectrum shows that the water molecules are rather mobile than deuterated 20-hydrate. This is come from the absence of the hydrogen bonding between water molecule.

Motional mode	T / K	Phase	Method	E_a / kJ mol^{-1}			
				29-Hydrate	Deuterated 20-hydrate	hexahydarte	deuterated hexahydrate
180° -flip	< 170	III	$T_1(^2H)$		16.5		
isotropic rotation (hydrated sphere)	172-240	II, III, IV	$T_1(^1H)$	25.9			
	> 230	I, II	$T_1(^2H)$		41.8		
	210-330	I, II	$T_1(^{23}Na)$	21.3			
diffusion of intermaediate water	> 270	I	$T_1(^1H)$	12.4			
	171-209	II, III	$\Delta\nu(^1H)$	26.5			

Table 2.2 The observed motion of the water molecule adsorbed in $Na_3PMo_{12}O_{40}$ crystal.

2.4 Conclusion

The static and dynamic properties of water molecules in $Na_3PMo_{12}O_{40} \cdot nH_2O$, with n =6 and 29, and in $Na_3PMo_{12}O_{40} \cdot nD_2O$, with n =6 and 20 were examined by NMR of ^1H, ^2H, and ^{23}Na in this chapter. The 29-hydrate and the deuterated 20-hydrate undergo four phase transitions below room temperature which may be associated with the change in the dynamic nature of the water molecules. The mobility of the crystallization water depends strongly on the hydration level as well as on temperature: The activation energy for several type of motional modes are listed in Table 2.2. The water molecules are highly mobile and form a "pseudoliquid phase" in the crystal lattice of the 29-hydrate in the highest temperature phase (Phase I) above 257 K. In this phase both the isotropic rotation and the translational diffusion are simultaneously activated. The Phase I of the deuterated 20-hydrate have also the pseudoliquid water, for which the activation energy for the isotropic rotation is considerably larger than that in the 29-hydrate due to the larger moment of inertia of the hydrated cation. In the second phase (Phase II between 190 and 257 K for 29-hydrate) the water molecules undergo isotropic rotation in both the 29- and the deuterated 20-hydrates. In the Phase III (between 180 and 190 K) two types of water molecules exist. One type is highly mobile even at 120 K and another almost rigid, reflecting the difference of the water sites with respect to the interaction between anions and cations and hydrogen bonding. It is noted that the "pseudoliquid" freezes at 190 K in the 29-hydrate and 200 K in the deuterated 20-hydrate which are the transition point between the Phases II and III.

In both the hexahydrate and the deuterated hexahydrate the water molecules undergo hindered motions due probably to interactions with the cations and/or anions of the host below room temperature down to 120 K; NMR spectra of ^{1}H and ^{2}H do not give any evidence of close interaction between water molecules such as hydrogen bonding. The result suggests that the number of the most stable (low energy), bound sites for water are limited to six per unit cell and these sites are far separated from each other, diminishing the direct interaction between water molecules. On increasing the hydration level water molecules occupy sequentially the sites with higher energies and form mobile clusters or hydration spheres around the Na^{+} ions. This finding will be of help to further studies of the catalytic activities of heteropoly compounds.

References for chapter 2

[1]H. S. Gutowsky, G. B. Kistiakowsky, G. E. Pake, and E. M. Purcell, *J. Phys. Chem.*, **17**(1949)972.

[2]M. Misono, *Catal. Rev.*,**29** (1987) 269.

[3] (a)A. Abragam, The Principles of Nuclear Magnetism, Clarendon Press, Oxford, 1961, ch. 8. (b)*ibid.*, ch. 7.

[4]G. M. Brown, M-R. Noe-Spirlet, W. R. Busing, and H. A. Levy, *Acta Crystallogr.*, B**33**(1977)1038.

[5] P. Waldstein, S. W. Rabideau, and J. A. Jackson, J. Chem. Phys., **41** (1964) 3407.

[6] K. Krynichi, Physica, **32** (1966) 167.

[7]O. Ya. Samoilov, Structura Vodnykh Rastvorov Elektrolitov I Gidrataciya Ionov, Moskva, 1957.

3. Catalytic reaction of methanol in $Na_3PMo_{12}O_{40}$ crystal

3.1 Experimental

$Na_3PMo_{12}O_{40} \cdot n CH_3OH$ was prepared by evaporation of the methanol solution of $Na_3PMo_{12}O_{40} \cdot 6H_2O$ under reduced pressure and the excess and part of adsorbed methanol was condensed onto the cold trap. The content of methanol was controlled by keeping the vapor pressure of methanol constant using a cold trap. ^{13}C enriched specimen was also prepared by similar method using ^{13}C enriched methanol by 20 % which was obtained by dilution of 99 atom% methanol-^{13}C (ISOTEC). Samples with n =6 and 9 were thus prepared. These specimens were placed in a teflon container and heated to 200 °C in the electric furnace to enhance the catalytic reaction of methanol. The specimens before and after heating were powdered and packed in zirconia rotor with Kel-F cap to measure ^1H and ^{31}P MAS and ^{13}C CPMAS NMR.

$Na_2HPMo_{12}O_{40}$ was prepared by neutralization of aq. solution of $H_3PMo_{12}O_{40}$ by stoichiometric Na_2CO_3; yellow crystals were obtained by evaporation of the solution. $Na_2HPMo_{12}O_{40} \cdot n CH_3OH$ was prepared from this crystal dried *in vacuo* by the same procedure as for trisodium salt. $Na_3PMo_{12}O_{40} \cdot n CH_3OCH_3$ was also prepared to identify the reaction product: Dimethylether gas was blown into the flask cooled by the liquid nitrogen to condense. Then the powder of $Na_3PMo_{12}O_{40} \cdot 6H_2O$ was dissolved in the liquid dimethylether and the specimen was obtained by evaporation of this solution at room temperature.

All NMR measurements were conducted by the use of Bruker MSL−200 and MSL−300 NMR system. The Larmor frequencies for ^{1}H, ^{13}C, and ^{31}P were 200.13 MHz, 50.32 MHz, and 81.01 MHz with MSL-200 system, respectively, and 300.13 MHz, 75.46 MHz, and 121.49 MHz respectively with MSL-300 system. The spin−lattice relaxation time of both ^{1}H and ^{31}P were short (< 100 ms). The chemical shift of ^{1}H was measured relative to external tetramethylsilane (TMS). Hexamethylbenzene and glycine were used to the external standard for ^{13}C chemical shift and converted to the TMS scale. The Hartmann-Hahn matching condition for cross polarization (CP) of ^{13}C was calibrated with glycine, and both CP (0.5 − 1 ms) and decoupling (10 − 40 ms) were performed at the same proton decoupling amplitude ($\omega_1/2\pi$ = 45.5 kHz) for both MSL-200 and MSL-300. FID accumulation by 8 scans with a 4 ms recycle delay were used to obtain the spectrum of the ^{13}C enriched specimen before heating whereas more than 10000 scans were needed for the specimen after heating. ^{31}P chemical shift was measured relative to external 85 % orthophosphoric acid.

3.2 Results

3.2.1 Content of methanol and X-ray diffraction

The content of methanol in the sodium 12-molybdophosphate crystal was determined by the gravimetric method as was used to determine the amount of the crystallization water in chapter **2**. The methanol content was controlled by adjusting the temperature of the cold trap which was used to keep the vapor pressure of methanol constant and to remove the excess methanol. The sample containing 9 molecules per anion was obtained by keeping the cold trap at 0°C. It took t about 1 week to achieve the equilibrium. On the other hand the sample containing 6 molecules per anion was obtained by using the trap kept in the vaporized liquid nitrogen. In this case the equilibrium achieved in a few hours. The sample with $n = 9$ were used for NMR measurements.

Fig. 3.1 shows the powder X-ray diffraction pattern of $Na_3PMo_{12}O_{40} \cdot 9CH_3OH$ at room temperature.

3.2.2 NMR spectra

The reaction process of methanol in $Na_3PMo_{12}O_{40}$ crystal has been traced by solid state ^{13}C, ^{1}H, and ^{31}P NMR. The ^{13}C static CP NMR spectrum of $Na_3PMo_{12}O_{40} \cdot 9CH_3OH$ at room temperature is shown in Fig. 3.2. It is likely consist of a sharp peak superposed by a broad signal. The chemical shift of the sharp peak is 52 ppm. The ^{13}C CPMAS spectrum of the same specimen shows a single sharp peak at 52ppm perhaps two shoulders at low field side at room temperature (Fig. 3.3). When this specimen was heated up to 50°C,

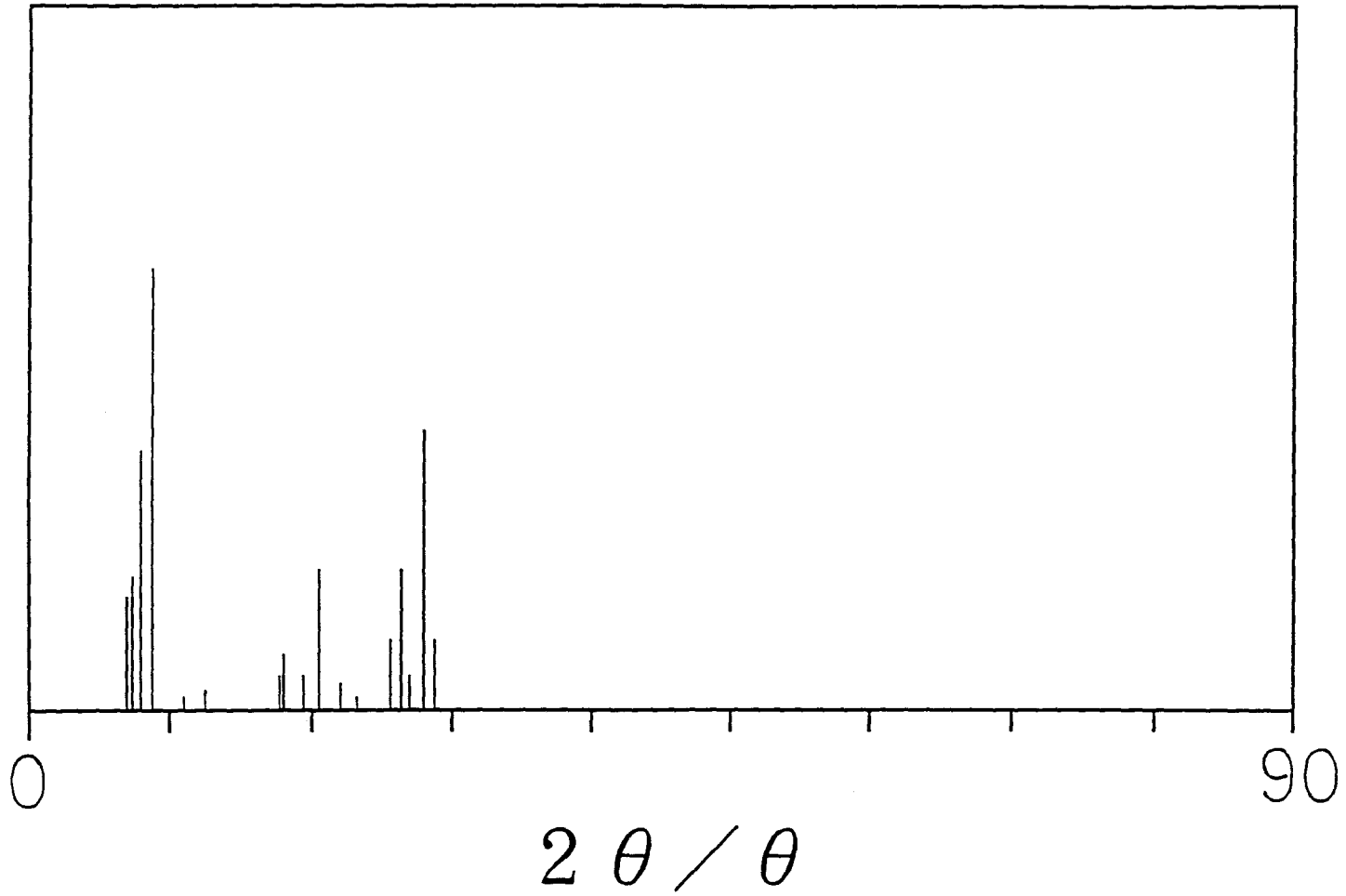

Fig. 3.1 The powder X-ray diffraction pattern of $Na_3PMo_{12}O_{40} \cdot 9CH_3OH$ at room temperature.

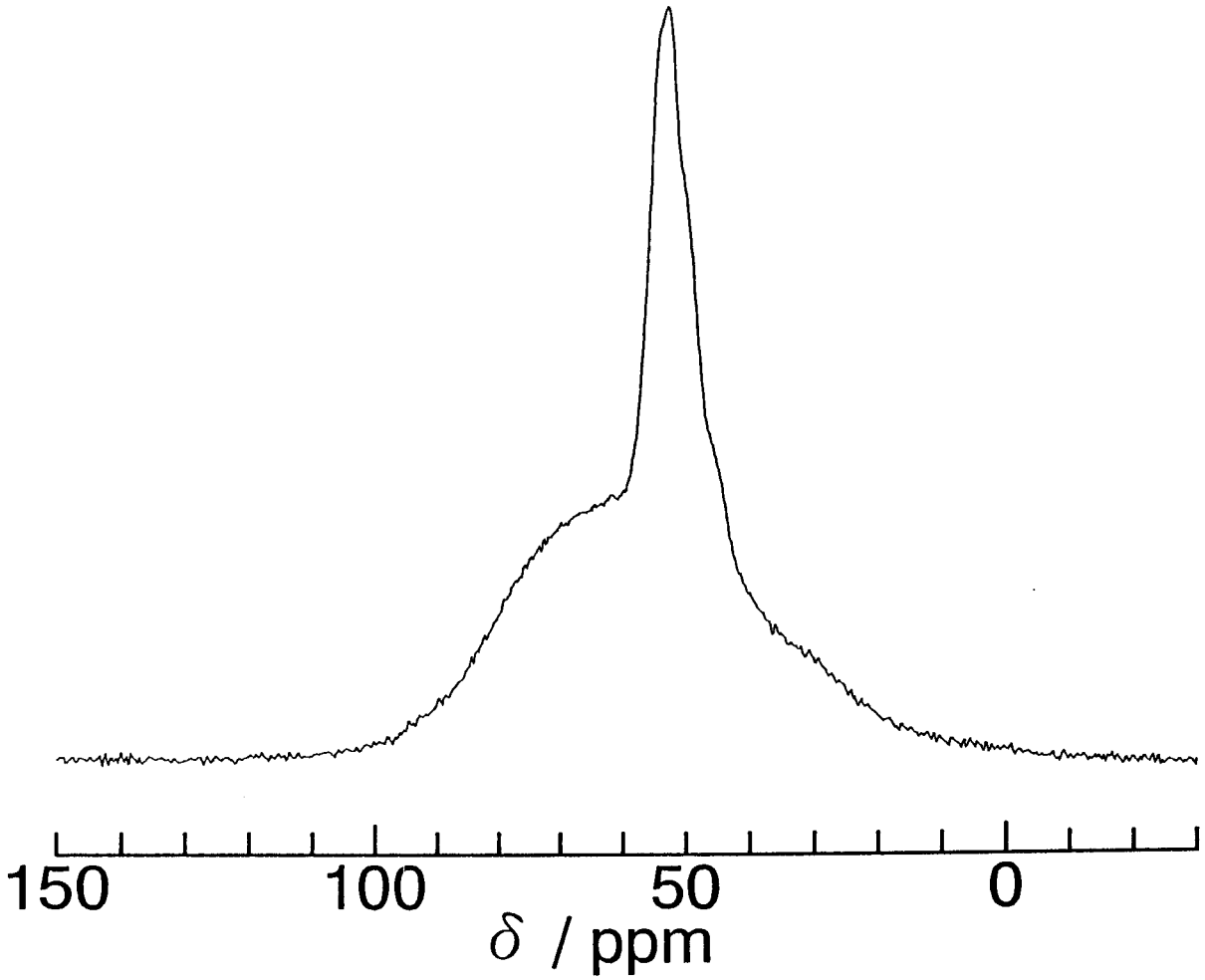

Fig. 3.2 ^{13}C static NMR spectrum of ^{13}C-enriched $Na_3PMo_{12}O_{40} \cdot 9CH_3OH$ at 50.32 MHz at room temperature.

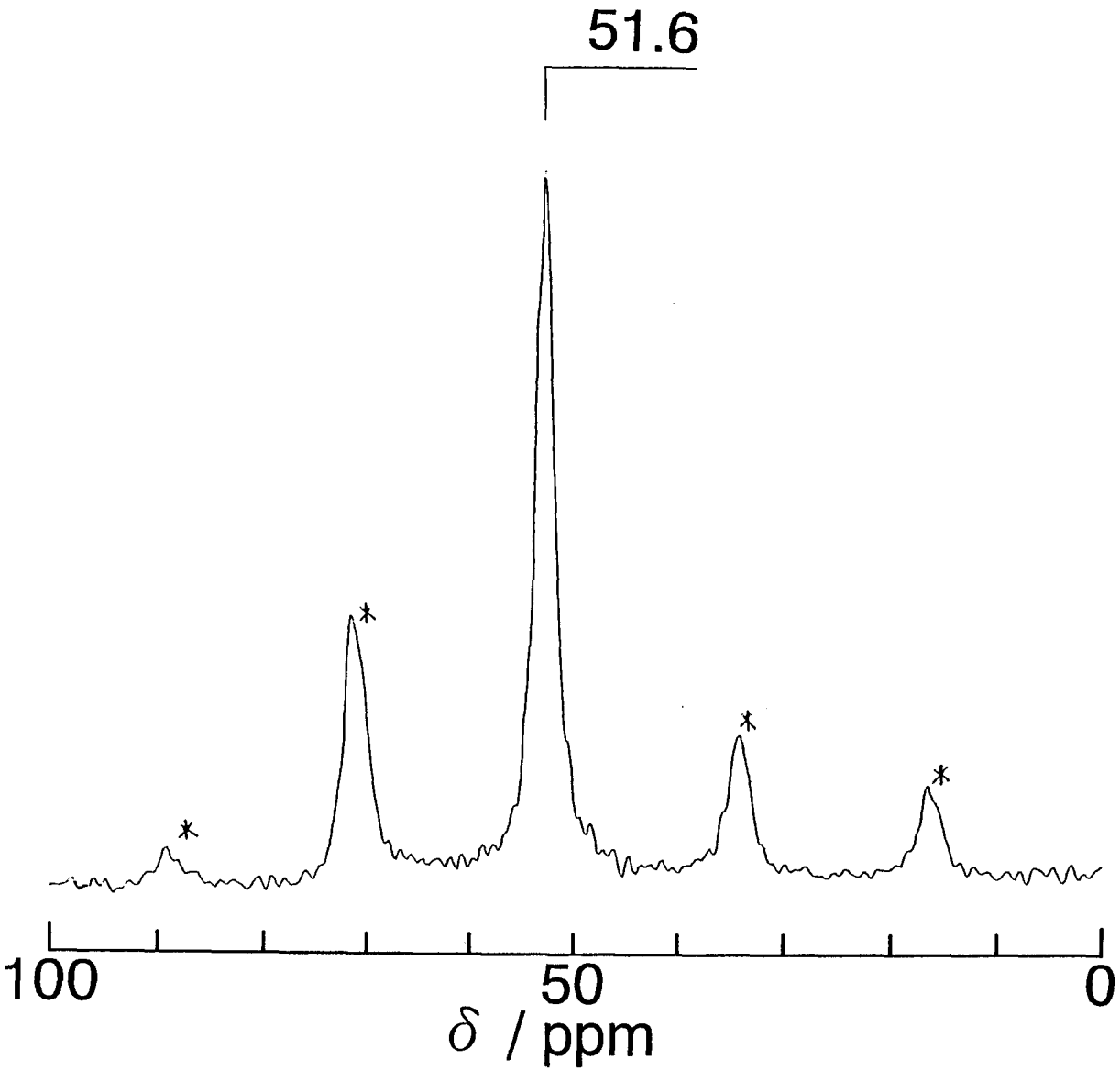

Fig. 3.3 ^{13}C CPMAS NMR spectrum of ^{13}C-enriched $Na_3PMo_{12}O_{40} \cdot 9CH_3OH$ at room temperature. The marked peaks (*) are the spinning side bands. The experimental conditions are as follows; Larmor frequency: 50.32 MHz, spinning rate: 1.47kHz, ^{13}C fraction: 20 %

the main peak splitted into two or three components. The peak position at the highest field coincide with that at room temperature and its chemical shift remains constant up to 100°C. On the other hand the other peaks shifted to the lower field, all peaks broadened, and their relative intensities increased with increasing temperature (Fig. 3.4). It seems that this change is almost reversible. On the other hand the spectrum of the sample which was once kept at 200°C for 1h in an electric furnace and cooled down to room temperature is much different (Fig. 3.5) from that of the sample before heating; the spectrum consists of considerably broad peaks at 52 ppm and 73 ppm and relatively sharp peak at 59 ppm. The change in the spectrum from one in Fig. 3.2 to Fig. 3.5 was irreversible, indicating some reaction of methanol proceeded at 200°C.

^{1}H NMR spectra were also measured to explore the mechanism of the above reaction. Comparatively sharp peaks were observed at room temperature in the broadline spectrum (static NMR, Fig. 3.6). Fig. 3.7a shows the ^{1}H MAS NMR spectrum of $Na_3PMo_{12}O_{40} \cdot 9CH_3OH$ at room temperature. A sharp peak and a broad peak were observed at 3.8 ppm and 6.7 ppm, respectively. The position of the broad peak at lower field was sensitive to the temperature. It shifted to higher field on heating as can be seen in Fig. 3.7b. After heating up to 200°C a sharp peak at 4.9 ppm and shoulder peak at 3.4 ppm appeared which were superposed by a very broad signal (Fig. 3.7c).

Fig. 3.8 and Fig. 3.9 show the ^{31}P static and MAS NMR spectrum, respectively, of $Na_3PMo_{12}O_{40} \cdot 9CH_3OH$ before and after heating at 200°C. The full width at half maximum of the static spectrum of the sample after heating considerably increased (14 ppm)

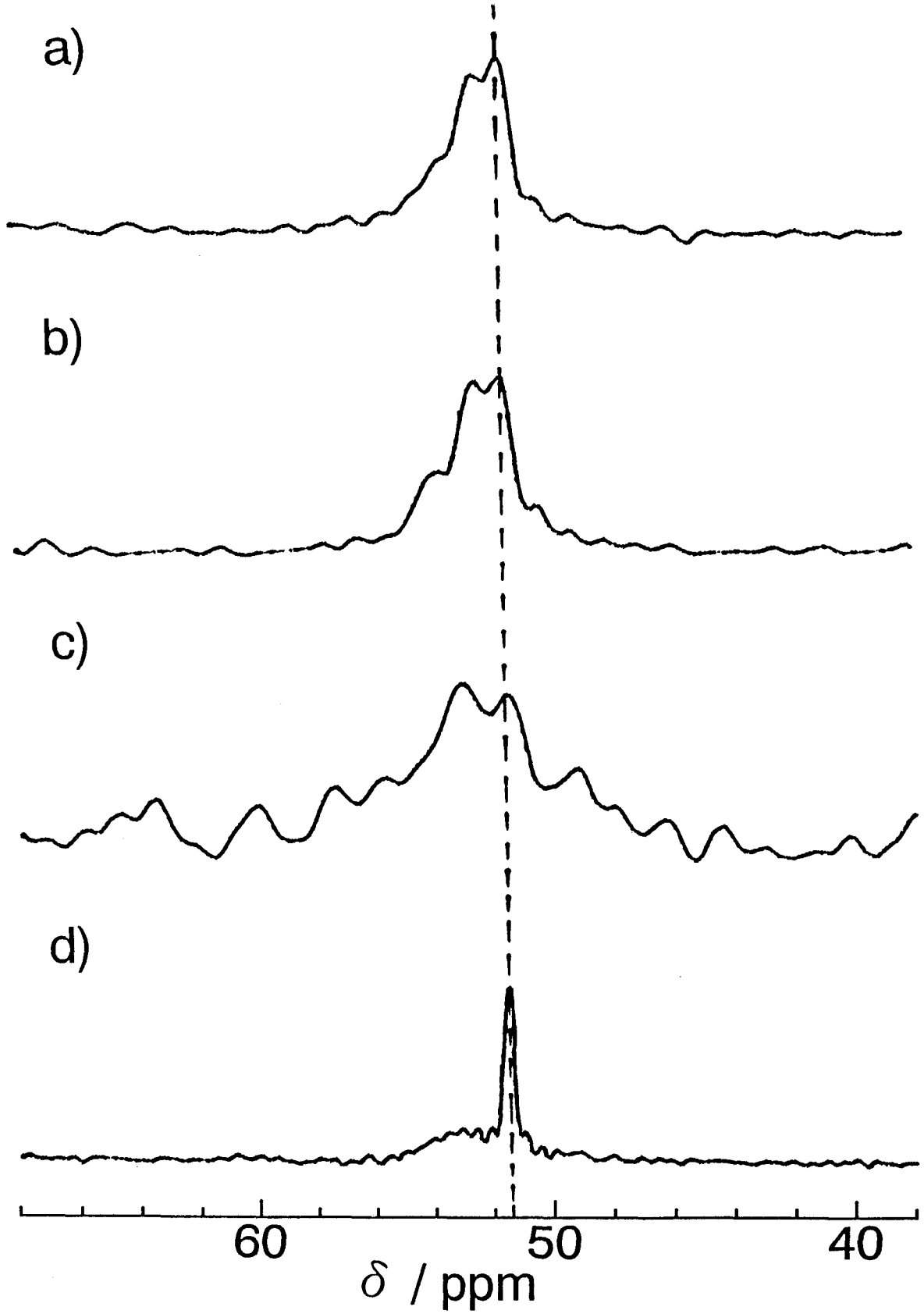

Fig. 3.4 The temperature dependence of the ^{13}C CPMAS spectrum of ^{13}C enriched $Na_3PMo_{12}O_{40} \cdot 9CH_3OH$: (a) 320 K, (b) 350 K, (c) 370 K, and (d) cooled down to room temperature again. The experimental conditions are as follows; Larmor frequency: 50.32 MHz, spinning rate: 900 Hz, ^{13}C fraction: 20 %

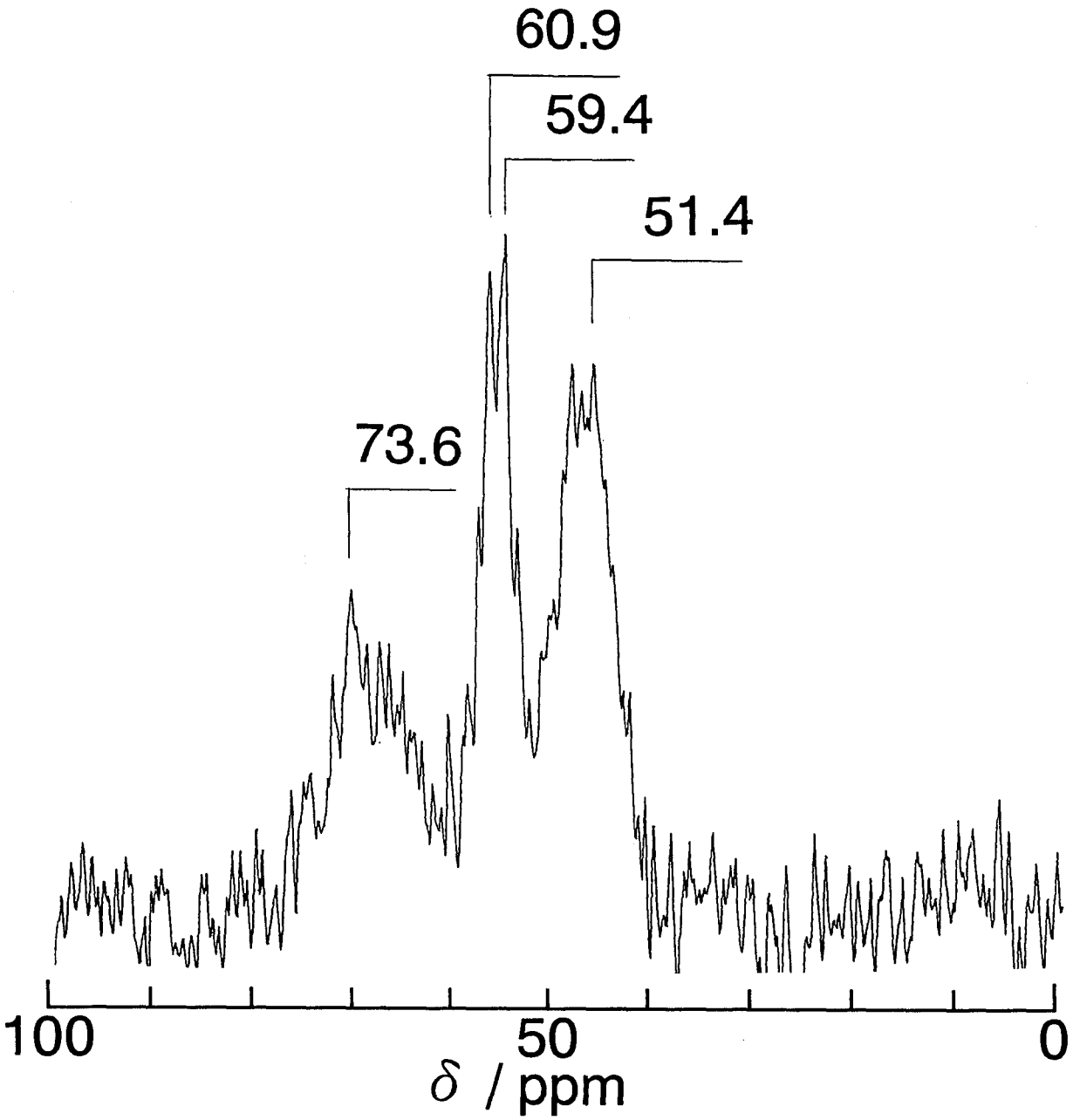

Fig. 3.5 Room temperature ^{13}C CPMAS spectrum of ^{13}C-enriched $Na_3PMo_{12}O_{40} \cdot 9CH_3OH$ which has been kept at 573 K for 1 hour. The experimental conditions are as follows; Larmor frequency: 75.46 MHz, spinning rate: 3.5 kHz, ^{13}C fraction: 20 %

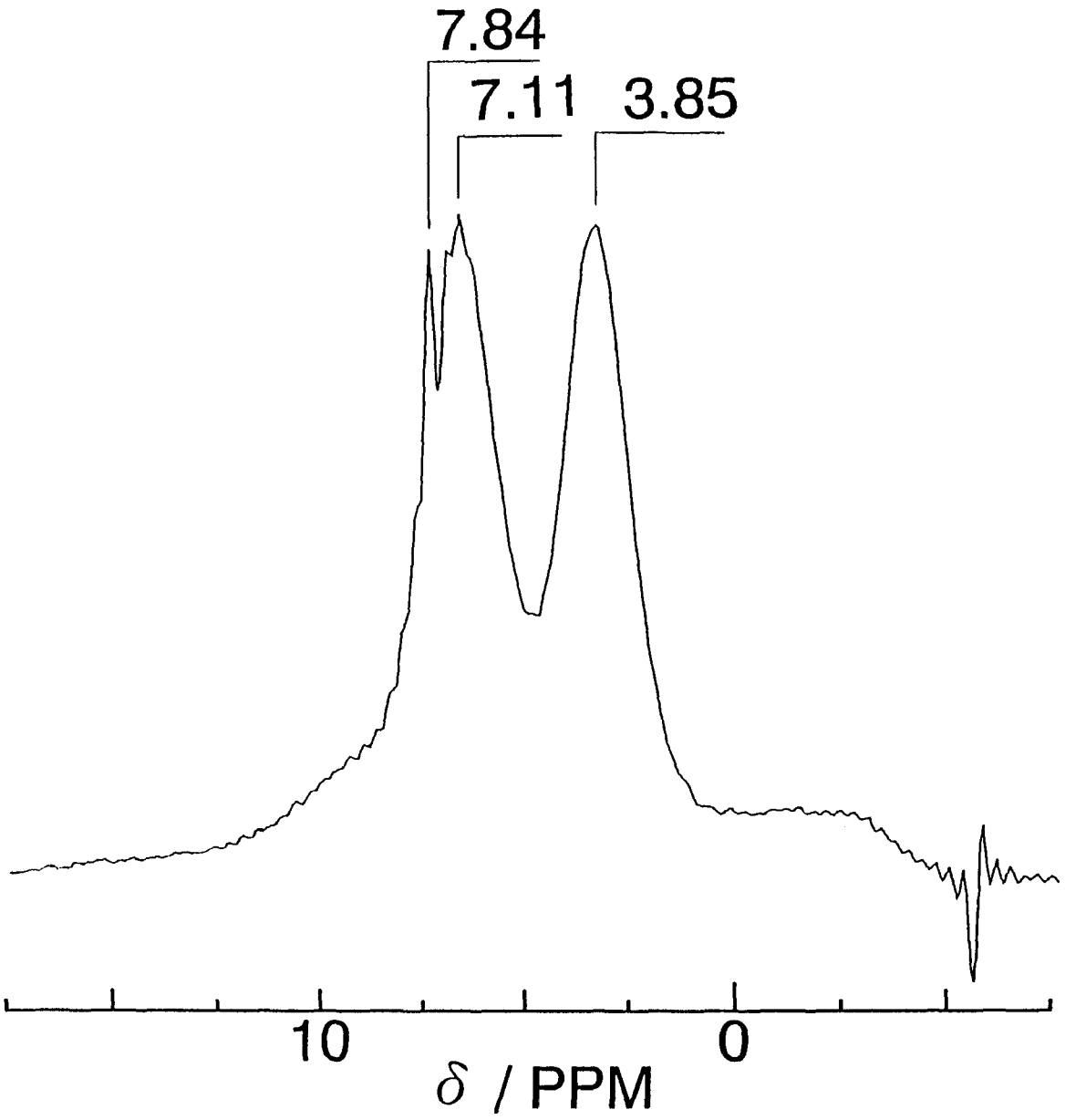

Fig. 3.6 ^{1}H static NMR spectrum of $Na_3PMo_{12}O_{40} \cdot 9CH_3OH$ at room temperature at Larmor frequency, 200.13 MHz.

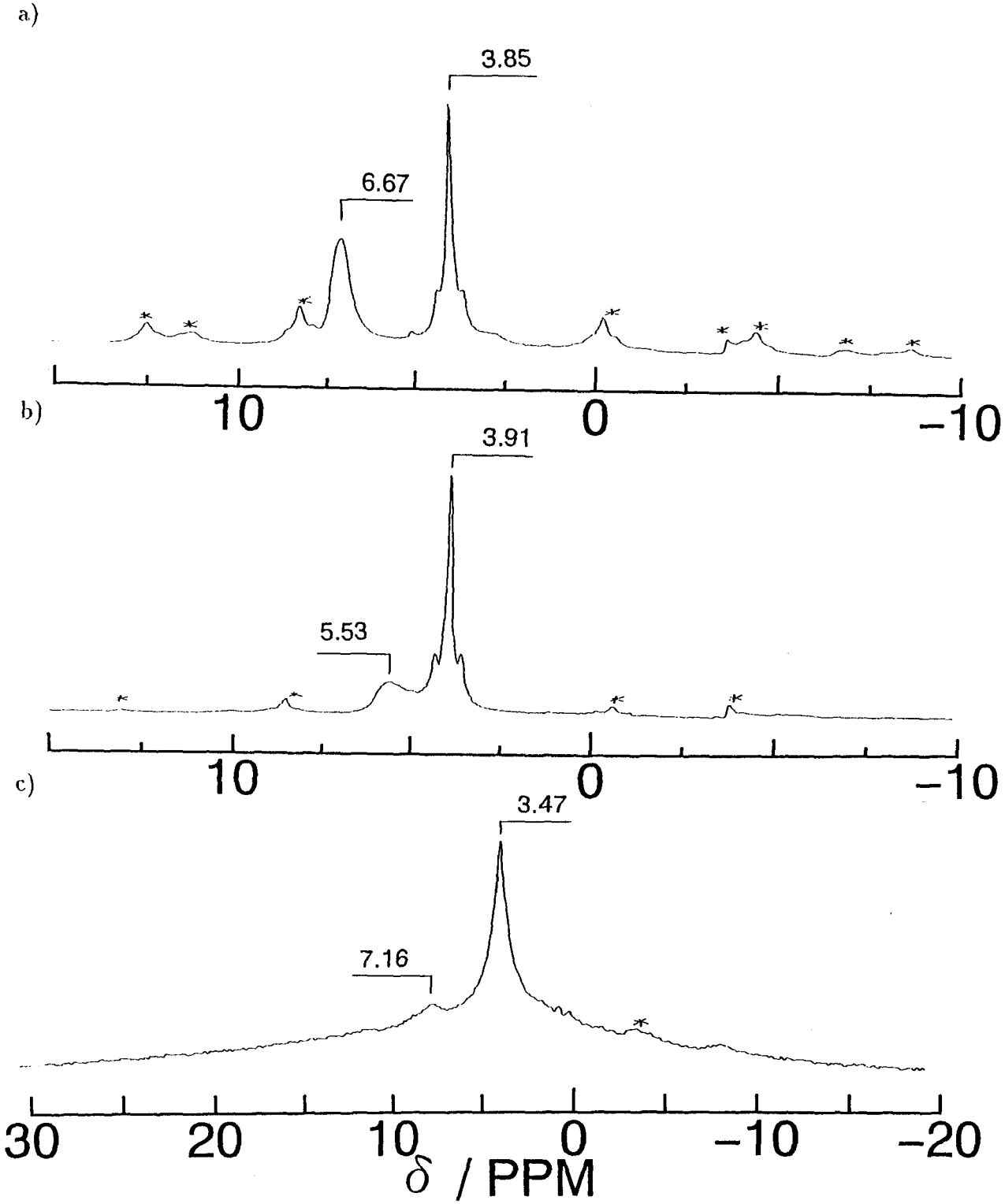

Fig. 3.7 ^{1}H MAS spectrum of $Na_3PMo_{12}O_{40}\cdot 9CH_3OH$ at Larmor frequency, 200.13 MHz. The experimental condition is as follows; (a)the spinning rate is 850 Hz at room temperature, (b)930 Hz at 320 K, and (c)1400 Hz after heated specimen. The two symmetric side peaks aside the sharp main peak are the splitted metyl proton by spin-spin coupling with the 20 % ^{13}C. The spinnig side bands are marked by *.

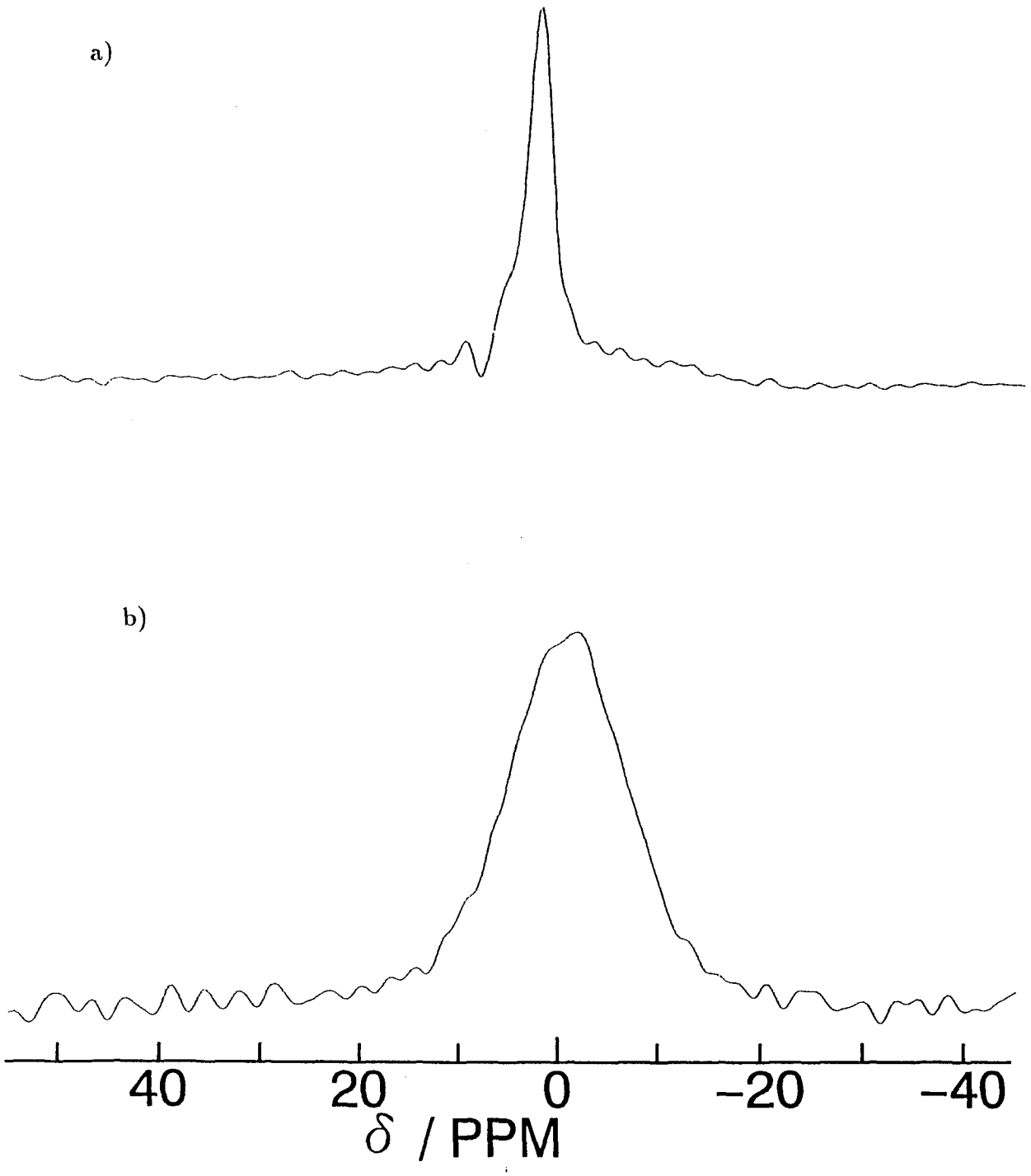

Fig. 3.8 ^{31}P broad-line NMR spectrum of (a)$Na_3PMo_{12}O_{40}\cdot 9CH_3OH$ at room temperature and (b)after heating specimen. Larmor frequency is 81.02 MHz and the X-axis calibrated to zero at each peak position.

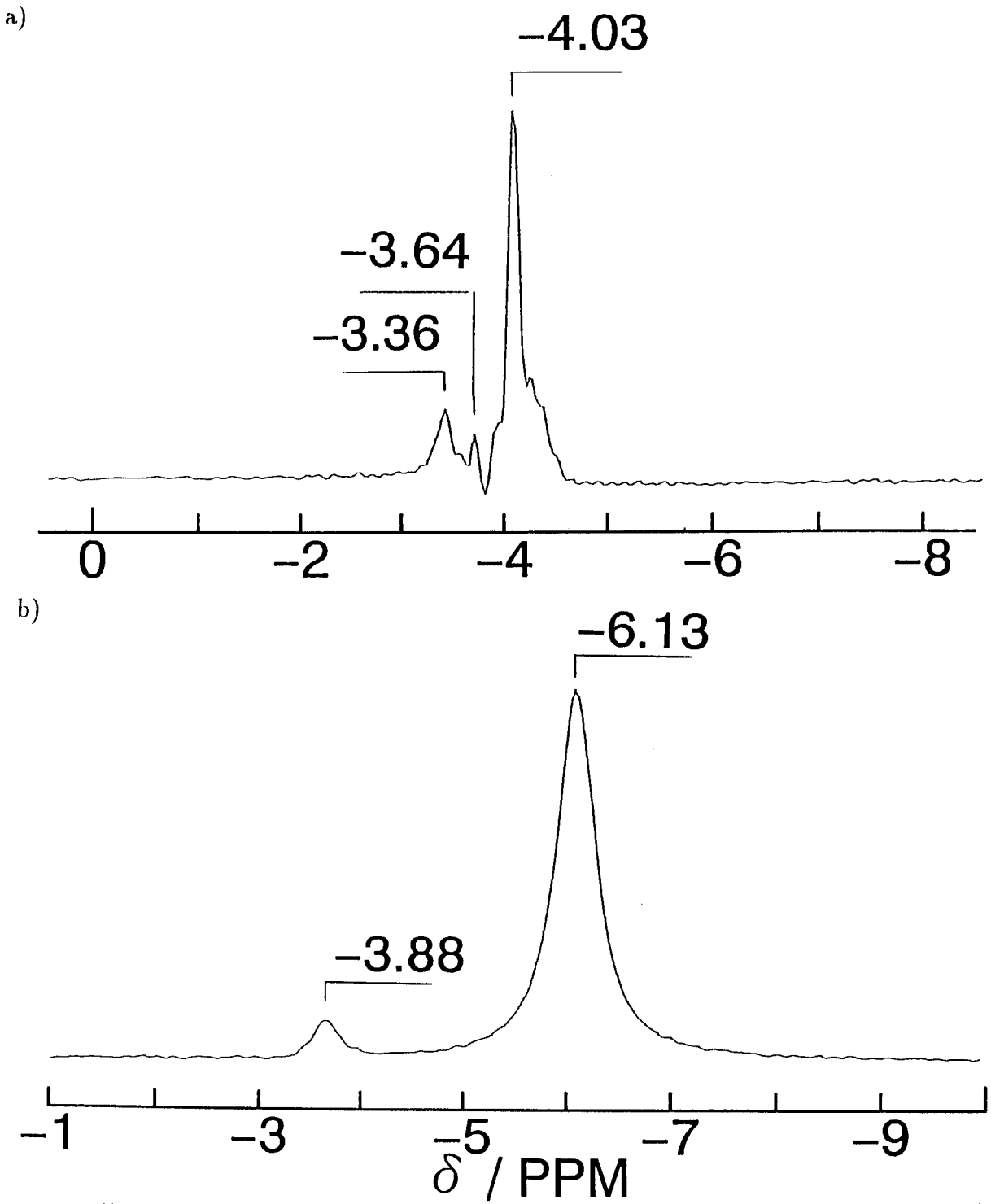

Fig. 3.9 ^{31}P MAS spectrum of (a) $Na_3PMo_{12}O_{40} \cdot 9CH_3OH$ at room temperature, and at the spinning rate is 4.1 kHz, and (b) after heating and at the spinning rate 2.9 kHz.

compared to that before heating (3.4 ppm). The MAS NMR spectrum of the sample before heating consists of a strong sharp peak at −4.0 ppm and some other small peaks. On the other hand two peaks were observed in the spectrum of the sample after heating at 200°C; main peak is at −6.1 ppm and small peak is at −3.7 ppm. These peaks are somewhat broader compared to the peaks in Fig. 3.9a before heating.

$Na_2HPMo_{12}O_{40}\cdot nCH_3OH$ were also prepared to investigate the effect of the existence of the acidic proton. ^{13}C CPMAS and ^1H MAS NMR spectra in this substance are shown in Fig. 3.10 and Fig. 3.11, respectively. ^{13}C CPMAS spectrum shows a peak at 53.0 ppm at room temperature. This peak shifts slightly to higher field compared to that in trisodium compound. In addition, a very broad peak centered at about 10 ppm was observed. ^1H MAS NMR gives a complicated spectrum: A sharp peak at 4.9 ppm and a broader one at 5.4 ppm were observed. Moreover, two shoulders appeared at 4.1 ppm and 8 ppm.

	Chemical shift / ppm		
	^{1}H	^{13}C	^{31}P
$Na_3PMo_{12}O_{40}$			
room temp.	3.8, 6.7 sharp broad	52 and two shoulders	-4.0 and three small peaks
200° C	4.9, 3.4 sharp shoulder	52, 59, 73 broad sharp broad	-6.1, -3.7
$Na_2HPMo_{12}O_{40}$			
room temp.	4.9, 5.4, 4.1, 8 sharp broad shoulder	53, ~60 very broad	

Table 3.1 The observed peaks by MAS NMR method for ^{1}H, ^{13}C, and ^{31}P of $Na_3PMo_{12}O_{40} \cdot 9CH_3OH$ crystal.

3.3 Discussion

3.3.1 Secondary structure of $Na_3PMo_{12}O_{40} \cdot n CH_3OH$

The powder X-ray diffraction pattern of $Na_3PMo_{12}O_{40} \cdot 9CH_3OH$ resembles that of $Na_3PMo_{12}O_{40} \cdot 6H_2O$ and the structure of the host framework is considered to be almost the same. This suggests that the guest molecules , *i.e.*, water or methanol, are absorbed into the space between the large anions and so the crystal structure is affected only slightly depending on the sort of the guest molecules at low absorption level. The methanol molecules are absorbed stepwise in particular molar ratio, *i.e.*, 6 or 9 molecules per anion, in $Na_3PMo_{12}O_{40}$ crystal by varying the vapor pressure of methanol. The numbers of methanol molecules are integral multiples of the number of sodium ions. This tendency is analogous to the case of crystallization water of $Na_3PMo_{12}O_{40}$. In other words methanol molecules in the crystal coordinate to the sodium ion and make up cluster like the solvation sphere in the solution. Similar property is observed with respect to the guests absorbed in 12-tungstophosphoric acid[1]. It is thought that the crystal structure is changed by increasing the gap between the ions for larger amount of the guest species and/or large guest molecules.

In the case of $Na_3PMo_{12}O_{40} \cdot n H_2O$ the guest molecules are distributed over various sites which have different binding energy to the guest H_2O molecule in the heteropoly crystal. In the case of $Na_3PMo_{12}O_{40} \cdot 9CH_3OH$ the ^{13}C static CP NMR spectrum consists of two components, one is sharp and centered at 52 ppm and another broad signal of which FWHM is about 40 ppm. This fact suggest that methanol molecules are also distributed

at least at two energetically different sites. Because the broad component merges into the sharp line when the magic angle spinning is applied to the sample, as stated later, the line broadening is caused certainly by the chemical shift anisotropy of the methanol and possibility of inhomogeneous broadening due to lattice imperfection is ruled out. It is therefore suggested that the methanol molecules which give broad component are tightly bound and so have low mobility whereas those correspond to the narrow component are loosely bound and highly mobile.

3.3.2 Analysis of the NMR spectra

The shielding constant is generally represented by the sum of the three terms,[2]

$$\sigma = \sigma^d + \sigma^p + \sigma',$$

where σ^d and σ^p are diamagnetic and the paramagnetic terms, and σ' represents contributions from neighboring atoms , interatomic currents and so on. The last term is usually very small and can be neglected in the present work. The σ^d is related to the electron density on the atomic nucleus in question and the σ^p is caused by the distortion from spherical symmetry of the electron cloud. For ^{1}H the chemical shift is governed by σ^d only and the range of the shift is limited to within about 10 ppm. On the other hand ^{13}C atom has three electrons in 2p orbitals which are largely apart from the spherical symmetry therefore the σ^p term become important and the range of the shift spread over about 200 ppm. The fact that ^{13} has such large chemical shift is of advantage to identification of the chemical species.

At first the feature of the ^{13}C and the ^{1}H NMR spectra of the methanol adsorbed are discussed. The observed ^{13}C CPMAS NMR spectrum of $Na_3PMo_{12}O_{40} \cdot 9CH_3OH$ consists of the single main peak centered at 52 ppm which accompanied by two or more shouldered components. However the differences of the chemical shift between these components are very small and so it can be regarded the spectrum as consisting of sharp peak. The value of the chemical shift of the main peak, 52ppm, is agrees well with 51 ppm in crystalline methanol[3], but somewhat large compared with that in the bulk liquid methanol, 47.1 ppm (Table 3.1). The ^{13}C CPMAS spectrum of $Na_2HPMo_{12}O_{40} \cdot nCH_3OH$ shows a peak at 53 ppm (see in Fig. 3.10). This value agrees well with the chemical shift of 51 ppm of methanol adsorbed in a heteropoly acid salt, $K_{3-x}H_xPMo_{12}O_{40}$.[4] The above ^{13}C chemical shift data suggest strongly that the sort of cations nor the degrees of acidity of the heteropoly system give significant effect on the ^{13}C chemical shift of the guest methanol molecule. The difference in chemical shift between the heteropoly materials and the bulk liquid methanol may come from the difference in the bulk magnetic susceptibilities.

The ^{1}H spectrum of adsorbed methanol in $Na_3PMo_{12}O_{40}$ consists of a single sharp peak at 3.9 ppm and a broad component at 7.1 ppm. The value of the chemical shift of the high field peak agrees approximately with the value of the methyl proton in the bulk methanol, 3.35 ppm. It is therefore assigned to the CH_3 group. However, another peak, which should be assigned to the hydroxyl proton and undesired residual water, appeared at very low field compared with the hydroxyl proton in the bulk methanol, 4.8 ppm, and the water proton, 4.6 ppm. Proton chemical shift can be a measure of degrees of the electron

transfer as mentioned above. Lee *et al.* reported a large shift (9.5 ppm) of the hydroxyl proton of ethanol absorbed in the 12-tungstophosphoric acid,[1] $H_3PW_{12}O_{40} \cdot 6C_2H_5OH$. They explained that this large shift is caused by the protonation of the acidic proton to the methanol molecule. In the case of $Na_3PMo_{12}O_{40}$ the acid proton responsible for the protonation is absent and therefore such mechanism can not have worked. It has been recognized that the hydroxyl and carboxylic protons which form strong hydrogen bonds give NMR signal at very low field[5]; it is therefore considered that the methanol molecule forms a strong hydrogen bond with, perhaps, large anion in the crystal lattice.

As can be seen in Fig. 3.4a-c the peak of ^{13}C CPMAS NMR spectrum splitted into three components on heating. The chemical shift of the main peak remained almost constant on heating but the other two components shifted to lower field with increasing the temperature. It is hardly possible to interpret such a type of temperature dependence of the chemical shift. Generally the methyl chemical shift in $CH_3 - O - X$ ranges between 48 ppm and 58 ppm[6], where X stands for various organic groups like -H, -CHO, -COOH, *etc.* Therefore it is difficult to consider that small change in the environment of the methanol due to temperature change brings about the significant down-field shift or shifts for particular methanol molecules. It has been known that the lineshape varies drastically in narrow temperature range when chemical exchange process take place. The phenomenon observed in the present work is regarded as an opposite process to the chemical exchange; it suggest therefore that some kind of recognization of the system or a cooperative phenomenon like phase separations takes place in the fleshly prepared 12-heteropoly inclusion complex. If

	δ / ppm	reference
liquid CH_3OH	47.1	
$Mo(OCH_3)_6$	64.0	a
$Na_4[Mo_8O_{24}(OCH_3)_4] \cdot 8H_2O$	69, 72	a
$[n-(C_6H_{13})_4N]_2OCH_3PMo_{12}O_{39}$	74.7	a
$K_xH_{3-x}OCH_3PMo_{12}O_{39}$	75.0	a
bond to HY-zeolite	55.7	b
bond to ZSM-5	60.7	c
CH_3OH in $Na_3PMo_{12}O_{40}$	52	This work
CH_3OH in $Na_2HPMo_{12}O_{40}$	53	〃
CH_3OCH_3 in $Na_3PMo_{12}O_{40}$	61	〃

(a) W. E. Farneth *et al.*, *J. Am. Chem. Soc.*, **109** (1987) 4018,(b) E. G. Derouane *et al.*, *J. Catal.*,**53** (1978) 40, (c) C. E. Bronnimann and G. E. Maciel, *J. Am. Chem. Soc.*, **108** (1986) 7154.

Table 3.2 ^{13}C chemical shift of methoxy carbon in various compounds.

such a process proceeds on heating some rearrangement of methanol molecule as well as the host framework which is accompanied by the down-field shift occurs and this dynamic rearrangement may be regarded as a sort of chemical exchange. At about 100°C the exchange the methanol molecules between the sites are enhanced, bringing about the line broadening. The phenomenon is reversible with respect to temperature cycle and can approximately be considered to be a simple thermal activation process.

After heating up to 200°C new ^{13}C peaks were observed at 59, 61, and 73 ppm in addition to the original main peak at 52 ppm as shown in Fig. 3.5. However the intensity of these peaks are very low because of loose of methanol by desorption and by remarkably line broadening. Dramatic change of the spectrum must be attributed to some catalytic reaction of methanol in crystal at 200°. It is noted, however, that the values of the chemical shift lie in the region of the ^{13}C chemical shift due to methoxy-carbons as summarized in Table 3.1. The broad highest field peak with the shift of 52 ppm can obviously be assigned to the original CH_3OH. The chemical shift of two closely spaced peaks, 59 and 61 ppm, may be attributed to dimethylether which was produced from methanol at on above 200°C in the $Na_3PMo_{12}O_{40}$ crystal. Indeed, it was confined in the present work that ^{13}C in dimethylether adsorbed in the $Na_3PMo_{12}O_{40}$ gives a signal at 61 ppm as in shown in Fig. 3.12. The splitting of the signal into two at 59 and 61 ppm may be attributed to some crystal field splitting at the CH_3 positions. The very broad peak at about 73 ppm can be assigned to the methoxy carbon which is directly bonded to the heteropoly anion; this is a sort of the ester of the heteropoly acid. It is surprising that neither a trace of aldehide

nor carboxylic acid detected after the catalytic reaction. The color of the specimen was changed from bright yellow to dark blue by heating it up to 200°C and by cooling down to room temperature. These color change indicates clearly that the heteropoly blue was produced by the reduction of the heteropoly anion; the 12-molybdophosphate is known to be reduced easily and in the present case a few among twelve Mo(VI) ions are reduced to Mo(V) or Mo(IV) without significant change of the anion structure[7]. This heterogeneous catalytic reduction of the heteropoly anion caused large inhomogeneous broadening of the peak of the methoxy carbon bonded to the anion because the unpaired electrons in the reduced specimens, Mo(V) or Mo(IV), brings about large chemical shift.

In order to examine the situation of the 12-heteropoly anions after the catalytic reaction the broadline and MAS NMR of ^{31}P were conducted. The ^{31}P chemical shift of some heteropoly compounds has distinct characteristics as can be seen in Table 3.2 which list the ^{31}P chemical shift values in various heteropoly compounds: 1) the chemical shift is almost independent of the sort of cation; 2) it is also independent of the number of the guest molecules; 3) clear up-field shift occurs when Mo is reduced. The ^{31}P MAS NMR spectrum of $Na_3PMo_{12}O_{40} \cdot 9CH_3OH$ at room temperature in Fig. 3.9a consists of a sharp main peak at -4.03 ppm and a few other small peaks around the main peak. These small peaks appeared probably due to some lattice distortion associated to the inclusion of the guest molecules. After heating up to 200°C the most part of the spectral components ^{31}P shifted to the value of -6.0 ppm, indicating that the most of the heteropoly anions were reduced to Mo(V) or to Mo(IV). It is noted that there still remain a small peak at 3.6

		δ / ppm	references
$PMo_{12}O_{40}^{3-}$	aquaous solution	-3.9	a
$PMo_9O_{34}^{9-}$		-1.4	b
$P_2Mo_{18}O_{62}^{6-}$		$-2.9 \sim -3.4$	a,c
$PMo_{11}O_{39}^{7-}$		-0.3	d
$PMo_{10}V_2O_{40}^{5-}$		$-3.1 \sim -3.8$	e
$PMo_{12}^{V,VI}O_{40}^{5-}$		-6	f
$PW_{12}O_{40}^{3-}$		-14.9	a,e
$H_3PMo_{12}O_{40} \cdot 30H_2O$	solid state	-3.9	g
$H_3PMo_{12}O_{40} \cdot 8H_2O$		-3.6	g
$Na_3PMo_{12}O_{40}$		-4.0	h
$K_3PMo_{12}O_{40}$		-4.4	h

(a) R. Massqrt *et al.*, *Inorg. Chem.*,**16** (1977) 2916, (b) T. Aoshima, *Thesis* (Faculty of Engenering, The University of Tokyo), (c) L. P. Kazansky and M. A. Fedotov, *J.C.S. Chem. Commun.*, **1980**, 644, (d) M. Ichida, *Thesis* (Faculty of Science, The University of Tokyo), (e) S. E. O'Donnell and M. T. Pope, *J.C.S. Dalton*, **1976**, 2290, (f) *Acta Crystallogr.*, **B31** (1975) 2688, (g) J. B. Black *et al.*, *J. Catal.*, **106** (1987) 1, (h) J. B. Black *et al.*, *J.C.S. Dalton*, **1984**, 2765.

Table 3.3 ^{31}P chemical shift of various heteropoly compounds.

ppm indicating the existence of unreduced heteropoly anion; this peak corresponding to the small peaks in the ^{31}P spectrum of the sample before heating (Fig. 3.9a).

The static (broadline) ^{31}P spectra in Fig. 3.8 evidenced that the reduction of Mo proceeded inhomogeneously: The virgin sample gave a narrow, relatively symmetric main absorption line, indicating that the phosphorus atom is located at the center of the spherical isotropic anion. There was detected no evidence for any defective Keggin structure such as $PMo_{11}O_{39}$. After heating up to 200° the absorption shifted up-field to the position of the signal of reduced heteropoly anion but its line width is extremely large. This fact means that the environment of the phosphorus is neither spherically symmetric nor axially symmetric. Such a asymmetry was certainly produced by reductions of Mo(VI) to Mo(V) or Mo(IV) at random in a large anion.

3.3.3 Mechanism of the reaction

It is known that the heteropoly compounds catalyze the oxidation reactions as mentioned before. It was also expected that $Na_3PMo_{12}O_{40}$ can be a good catalyst for similar reactions. However this work revealed that $Na_3PMo_{12}O_{40}$ crystal has catalytic activity for only the etherification of methanol; this work did not detected even trace of the carboxyl or carbonyl compounds which should be reaction products of the oxidation of the alcohol. Probable reason why oxidation does not occur in the crystals of $Na_3PMo_{12}O_{40}$ is as follows:

1) Acidic protons are essential for the catalytic oxidation,

2) Continuous supply of gaseous oxygen is necessary.

The condition 1) can be examined by repeating reactions under the same experimental conditions as in the present work by using $Na_{3-x}H_xPMo_{12}O_{40}$. As to the second condition the present reaction was carried out in a closed system without of oxygen supply. In practice, special reaction vessel will have to be designed for supply gaseous oxygen into the sample at high temperature and at high pressure without losing methanol or reaction products by desorption and it will be a future project.

The last point in this work is to think about the mechanism of the conversion of the methanol to dimethylether. A mechanism for the etherification of the methanol catalyzed by $K_xH_{3-x}PMo_{12}O_{40}$ has been proposed as shown in scheme 1.[4] Similar mechanism was also supported for the formation of ethylene from ethanol with $H_3PW_{12}O_{40}$ as the catalyst.[1] The existence of intermediate like **2** was supported by the ^{13}C CP-MAS NMR in present work. Thus it is likely that the dimethylether is also formed from $Na_3PMo_{12}O_{40} \cdot 9CH_3OH$ by similar mechanism, if the intermediate **1** can be formed in the absence of acid protons. In the present work there is a possibility that some trace of water remain in the crystal sample of $Na_3PMo_{12}O_{40}$ after rigorous dehydration prior to alcoholization of the sample. Then the water plays a role to produce **1** in a step given in Scheme 2.

Another possible mechanism for etherification of alcohol is proposed as shown in Scheme 3. In this scheme the reaction is driven by the oxidizing activity of the heteropoly anion Mo(VI) in a heteropoly anion take an electron away from a

and is reduced to Mo(V), and meanwhile the methanol cation radical is bound to this Mo(V), forming the intermediate **2**. This mechanism is promising since a species which corresponds to **2** has been detected in the present ^{13}C CPMAS experiment. The former mechanism contains the formation of defected Keggin anion like $PMo_{11}O_{39}^{7-}$, however no evidence for such a hydrolyzed heteropoly anion was detected by the present ^{31}P NMR. On the other hand ^{1}H MAS NMR of $Na_3PMo_{12}O_{40} \cdot 9CH_3OH$ found a large down-field shift of the hydroxyl proton. This fact suggests that the hydroxyl carbon forms a strong hydrogen bond with some active site in the large anion. This is also a possibility that a complex given in the scheme 3 between Mo and methanol. The anomalous down-field shift of the hydroxyl proton as well as anomalous broadening the spectrum may be accounted for by the complex formation

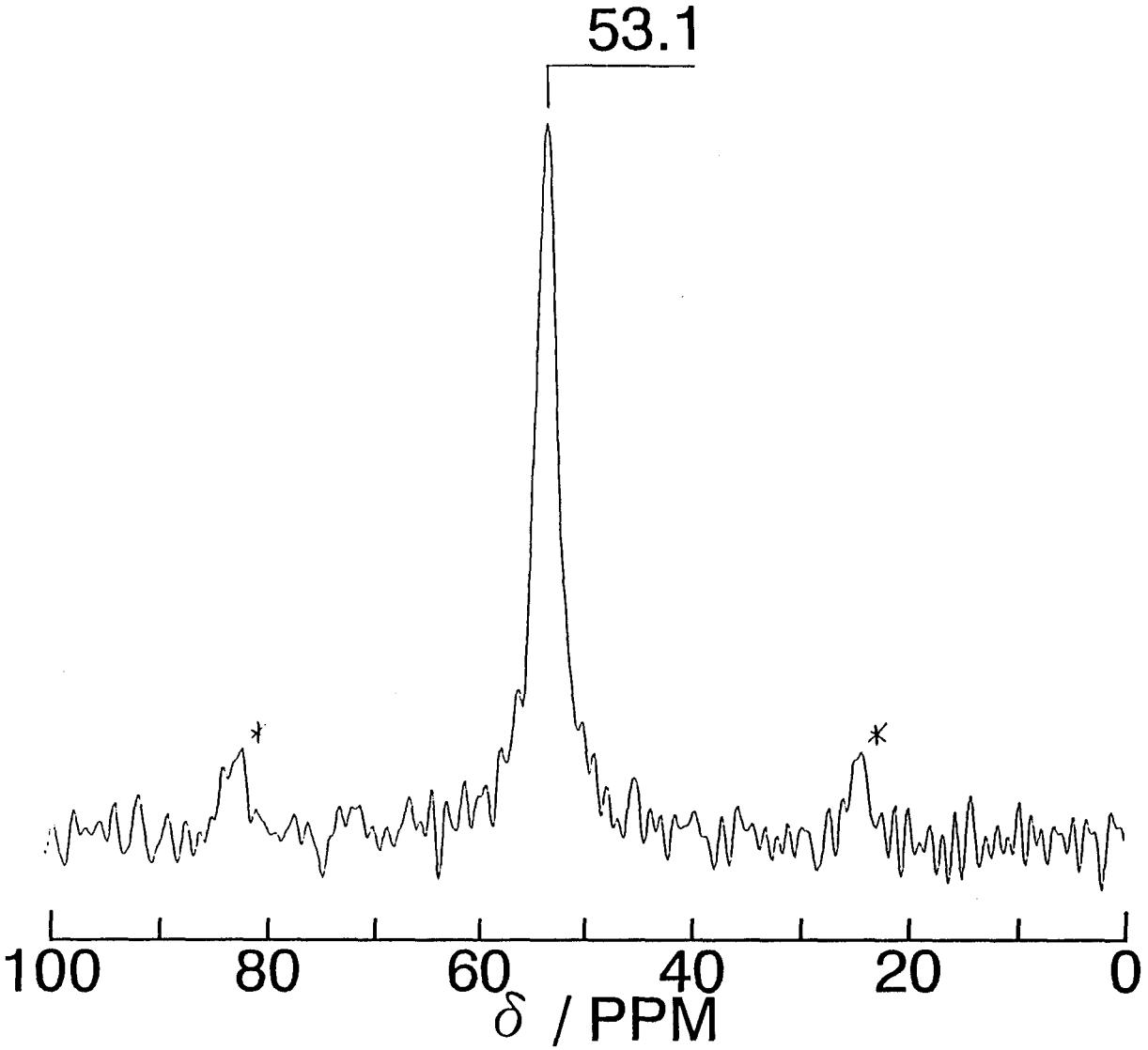

Fig. 3.10 ^{13}C CPMAS spectrum of ^{13}C enriched $Na_2HPMo_{12}O_{40} \cdot n CH_3OH$ at room temperature. The spinning rate is 3.6 kHz and Larmor frequency is 75.47 MHz.

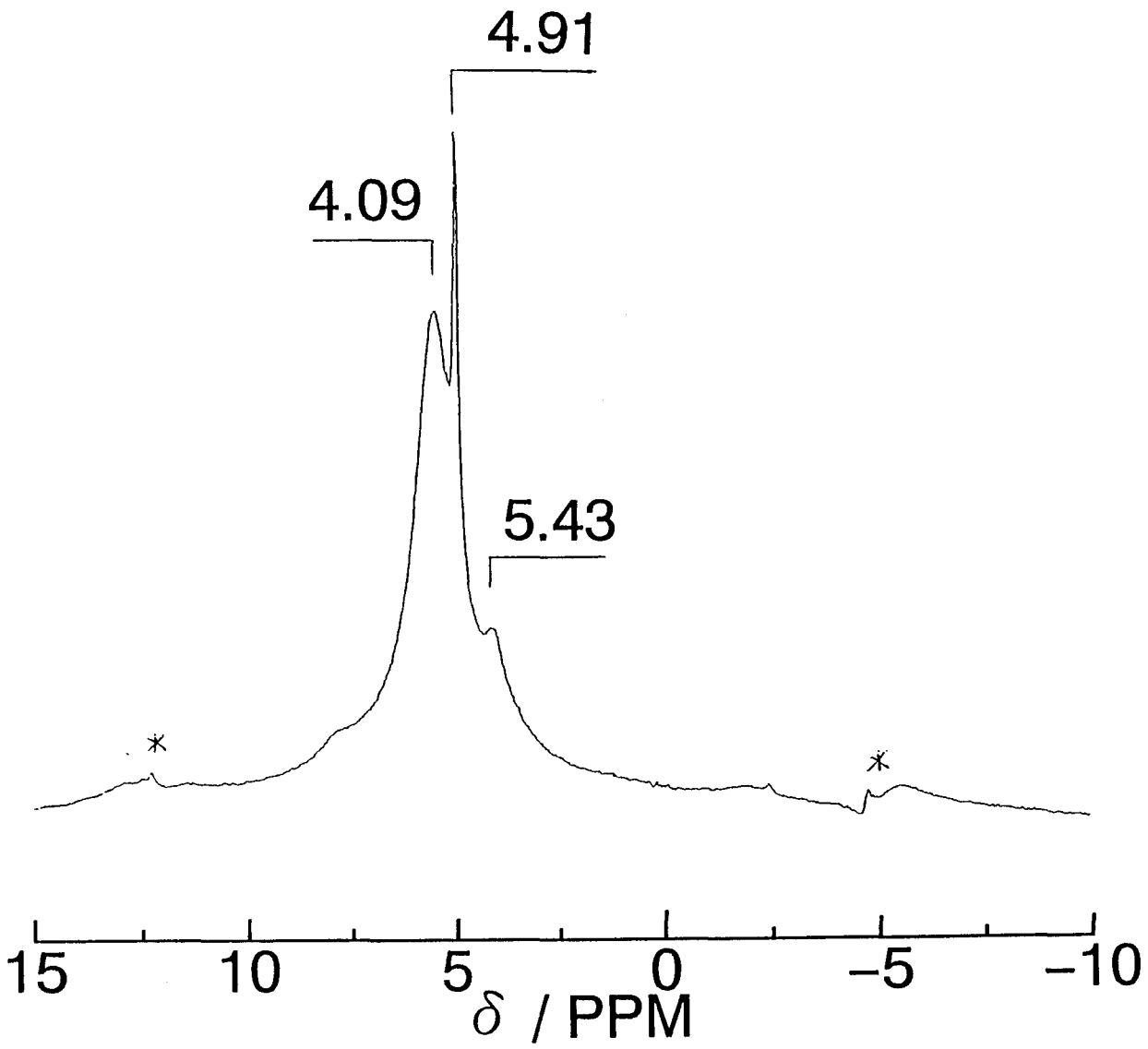

Fig. 3.11 ^{1}H MAS NMR spectrum of ^{13}C enriched $Na_2HPMo_{12}O_{40} \cdot nCH_3OH$ at room temperature at spinning rate, 1.5 kHz and larmor frequency, 200.13 MHz. The spinning side band is marked by *.

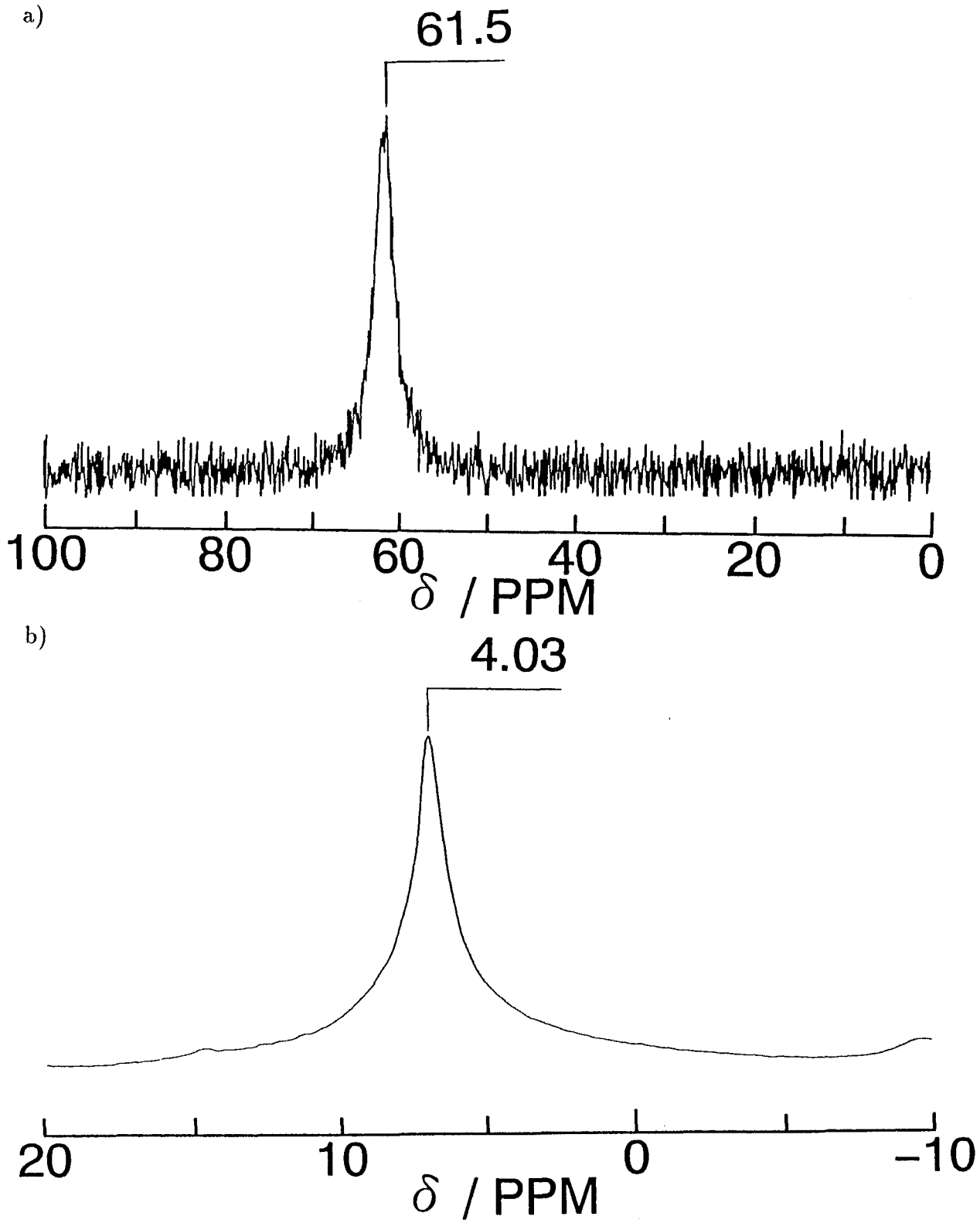

Fig. 3.12 The NMR spectrum of $Na_3PMo_{12}O_{40}\cdot nCH_3OCH_3$ at room temperature; (a)^{13}C CPMAS at the spinning rate 4.0 kHz and Larmor frequency 75.47 MHz, and (b)^1H MAS at the spinning rate 2.8 kHz and Larmor frequency 300.13 MHz.

3.4 Conclusion

In this chapter the dynamic structure and the reaction of the methanol, which is one of the simplest organic compounds, absorbed in trisodium 12-molybdophosphate were investigated by solid state ^{1}H, ^{13}CP/MAS, and ^{31}P MAS NMR measurements. It was found that the materials $Na_3PMo_{12}O_{40} \cdot nCH_3OH$ where n= 6 and 9 could be obtained from the methanol solution of dehydrated trisodium 12-molybdophosphate by evaporating the solvent methanol. The methanol content was controled by adjusting the vapor pressure of methanol. ^{13}C broadline NMR spectrum of adsorbed methanol consists of two components; one is attributed to relatively free and mobile methanol and another to bound tightly to the host. This is analogous to the ocasion for the adsorbed water as mentioned in Chapter 2. The powder X-ray diffraction of n = 9 specimen at room temperature also shows almost the same pattern as that for hexahydrate, $Na_3PMo_{12}O_{40} \cdot 6H_2O$, indicating that the structure of the host framework is not sensitive to the sort of the guest.

The methanol adsorbed in trisodium salt and in disodium salt, $Na_2HPMo_{12}O_{40}$, gave almost the same ^{13}C CPMAS spectra. The ^{13}C CPMAS spectrum was changed dramastically by heating $Na_3PMo_{12}O_{40} \cdot 9CH_3OH$ up to 200°C in closed vessel. It consists of a couple of a new singla components at 60 ppm and 74 ppm, and of a weak component at 51 ppm corresponding to the original methanol molecules. The first component 60 ppm is due obviously to dimethylether which was produced by a oxidation reaction catalyzed by $[PMo_{12}O_{40}]^{3-}$ anion. The second component at 74 ppm can be assigned to a reaction intermediate the structure of which may be somewhat like CH_3O-Mo=. The hetropoly

anion was partly reduced by this reaction, indicating that it possesses strong oxidizing activity.

The catalytic etherification in a heteropoly compound was explored by the present work for the first time; a new mechanism for this reaction was proposed on the basis of the present NMR results.

References for chapter 3

[1]K. Y. Lee, Y. Kanda, N. Mizuno, T. Okuhara, M. Misono, S. Nakata, and S. Asaoka, *Chem. Lett.*, **1988**,1175.

[2]C. P. Slichter, Principle of Magnetic Resonance, 3rd Ed., Splinger-Verlag, Berling, 1989, Chapter 4.

[3]A. Pines, M. G. Gibby, and J. S. Waugh, *Chem. Phys. Lett.*, **15**(1972)373.

[4]W. E. Farneth, R. H. Staley, P. J. Domaille, and R. D. Farlee, *J. Am. Chem. Soc.*, **109**(1987)4018.

[5]F. D. Becker, High Resolution NMR, 2nd Ed., New York, 1980, Chapter 12.

[6]W. S. Veeman, *Progr. NMR Spectrosc.*, **16**(1984)193.

[7]B. K. Hodnett, and J. B. Moffat, *J. Catal.*, **91**(1981)83.

4. Summary

It has recently recognized that solid state NMR can be one of the most useful tools for exploring the structure and dynamics of the molecules adsorbed on catalytic materials. The solid state NMR methods have also been applied to trace some catalytic reactions *in situ* and brought about a number of promising results. This work has been planed to apply various solid state NMR techniques to the study of the dynamic structure of guest molecules, the microscopic nature of the guest-host interaction, and the mechanism of possible catalytic reaction of guest materials in a series of 12-heteropoly compounds which have recently been pained attention as a new kind of strong oxidizing agents.

Two systems, *i.e.*, $Na_3PMo_{12}O_{40}\cdot nH_2O$ and $Na_3PMo_{12}O_{40}\cdot nCH_3OH$ were chosen as the subject of the present work. These materials are both very basic subjects for examining the static and dynamic behavior of adsorbate molecules from the microscopic of point of view and especially the latter will be the fundamental materials for investigating the catalytic activity of the heteropoly compounds. In order to study these systems a variety of the solid state NMR techniques were applied and the usefulness of these methods were discussed. The methods being applied to the hydrate system are broadline spectrum and the spin-lattice relaxation measurements of ^1H and ^{23}Na. These methods were combined successfully to derive information on the specific active sites in the host lattice, the variation of motional states of the H_2O molecules over wide temperature range, the nature of the host-guest interactions, and the interrelation between the motional states of water molecules and successive phase transitions which occur in the material. Broadline and high-resolution

NMR techniques such as MAS and CPMAS on ^{1}H, ^{13}C, and ^{31}P were applied to trace the catalytic reaction of the methanol inclusion complex. It was found that methanol converts into dimethylether at about 200°C. ^{13}C CPMAS method revealed clearly that this reaction proceeds via an intermediate reaction complex CH_3O-Mo=, the fact that Mo(VI) is reduced in the process of the reaction by ^{31}P broadline and MAS spectrum. A possible mechanism for the catalytic oxidation of methanol was proposed for the first time in this work. This work thus establishes an important methodology for the study of heterogeneous catalytic reactions *in situ* by the solid state NMR techniques.